

A Well-Tempered Landscape for Non-convex Robust Subspace Recovery

Tyler Maunu

*School of Mathematics
University of Minnesota
Minneapolis, MN 55455*

MAUN0021@UMN.EDU

Teng Zhang

*Department of Mathematics
University of Central Florida
Orlando, FL 32816*

TENG.ZHANG@UCF.EDU

Gilad Lerman

*School of Mathematics
University of Minnesota
Minneapolis, MN 55455*

LERMAN@UMN.EDU

Editor:

Abstract

We present a mathematical analysis of a non-convex energy landscape for Robust Subspace Recovery. We prove that an underlying subspace is the only stationary point and local minimizer in a large neighborhood if a generic condition holds for a dataset. We further show that if the generic condition is satisfied, a geodesic gradient descent method over the Grassmannian manifold can exactly recover the underlying subspace with proper initialization. The condition is shown to hold with high probability for a certain model of data.

Keywords: Robust Subspace Recovery, Non-convex Optimization, Dimension Reduction, Optimization on the Grassmannian

1. Introduction

An essential tool in any data analysis toolbox is Principal Component Analysis (PCA) (Jolliffe, 2002). PCA is popular for both reducing noise and capturing low-dimension structure within data. However, it is often quite challenging to locate such structures when the data is corrupted.

The basic problem formulation for PCA can be cast as an optimization problem over the Grassmannian manifold of d -dimensional linear subspaces in \mathbb{R}^D : we denote this set by $G(D, d)$. For a dataset $\mathcal{X} = \{\mathbf{x}_1, \dots, \mathbf{x}_n\}$ centered at the origin, the PCA d -subspace is the solution of the least squares problem

$$\min_{L \in G(D, d)} \sum_{i=1}^N \|\mathbf{x}_i - P_L \mathbf{x}_i\|_2^2,$$

where \mathbf{P}_L denotes the orthogonal projection onto the subspace L . Due to the non-convexity of $G(D, d)$, we see that PCA is a non-convex problem. However, despite non-convexity, PCA has a closed form solution, which can be calculated from the singular value decomposition of the data matrix $\mathbf{X} = [\mathbf{x}_1, \dots, \mathbf{x}_n]$. The PCA optimization also has a nice energy landscape. Indeed, if the d th singular value of \mathbf{X} is larger than the $(d + 1)$ st singular value, then the global minimum is unique, and there are no other local minima; otherwise, all local minima are globally optimal. Saddle points are also guaranteed to be sufficiently far from the global minimum, and they have closed form expressions.

As has been noted in many past works (Osborne and Watson, 1985; Späth and Watson, 1987; Nyquist, 1988; Watson, 2001; Ding et al., 2006; McCoy and Tropp, 2011; Xu et al., 2012, 2013; Zhang and Lerman, 2014; Lerman et al., 2015; Lerman and Maunu, 2014), the least squares formulation is sensitive to outliers. By inliers and outliers, we mean points that lie near a low-dimensional subspace and points that do not, respectively. To make this optimization more robust, one may instead try to solve

$$\min_{L \in G(D, d)} \sum_{i=1}^N \|\mathbf{x}_i - \mathbf{P}_L \mathbf{x}_i\|_2. \quad (1)$$

This sort of formulation, known as least absolute deviations (Osborne and Watson, 1985; Watson, 2001; Ding et al., 2006; Lerman et al., 2015), has been around for a long time. The idea of least absolute deviations for orthogonal regression was introduced by Osborne and Watson (1985) but was not extended to PCA until much later (Watson, 2001; Ding et al., 2006). Previous works have considered convex relaxation of this cost (McCoy and Tropp, 2011; Xu et al., 2012; Zhang and Lerman, 2014; Lerman et al., 2015). The work of Lerman and Maunu (2014) attempted to directly minimize the non-convex cost.

Minimizing this function involves solving a non-convex optimization problem, which can be hard in general. We give examples of two simulated energy landscapes in Figure 1. The novelty of this paper consists of the following observation about the energy landscape of (1): in Figure 1, despite non-convexity, the energy landscape appears to be nice around underlying subspaces. In this work, we are able to offer the first generic condition which guarantees nice behavior of the non-convex energy landscape around an underlying subspace. We show that this condition also ensures local exact recovery of a subspace with a geodesic gradient descent method. Further, we are able to show that a data model satisfies this condition with high probability, and thus our Algorithm is guaranteed to succeed with this model for large enough samples. To our knowledge, we give the strongest guarantees on a non-convex method for Robust Subspace Recovery to date and even obtain stronger results than some convex methods.

2. Previous Work

We focus on robust subspace estimation in the presence of wholly corrupted samples. This is distinctly different from what is typically called robust Principal Component Analysis (Candès et al., 2011), which focuses on elementwise corruption of the entire data matrix. Estimation in the presence of sample outliers is typically referred to as Robust Subspace Recovery (RSR), and examples of works on this topic include Maronna (2005); Maronna et al. (2006); Ding et al. (2006); Zhang et al. (2009); McCoy and Tropp (2011); Xu et al.

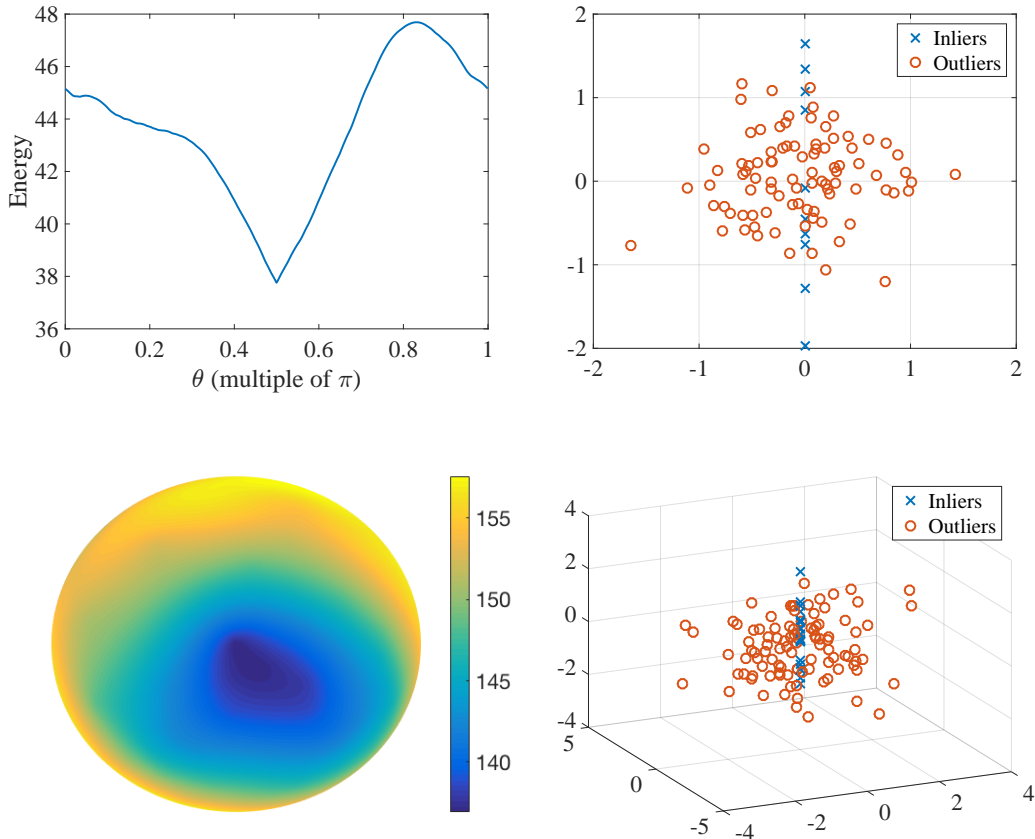


Figure 1: Demonstration of the energy landscape of (1) over $G(2, 1)$ and $G(3, 1)$ with simulated Gaussian data. Top: In \mathbb{R}^2 , 90 outliers are i.i.d. $\mathcal{N}(\mathbf{0}, \mathbf{I}/2)$ and 10 inliers are i.i.d. $\mathcal{N}(0, 1)$ along the y -axis. $G(2, 1)$ is identified with the top of the unit circle and parametrized by angle. The global minimum is at $\pi/2$, that is, at the y -axis. Bottom: In \mathbb{R}^3 , 100 outliers are i.i.d. $\mathcal{N}(\mathbf{0}, 4\mathbf{I}_3/3)$ and 20 inliers are i.i.d. $\mathcal{N}(0, 1)$ along the z -axis. $G(3, 1)$ is identified with the top hemisphere which is flattened to a circle. The global minimum is at the center of the circle, that is, at the z -axis.

(2012); Coudron and Lerman (2012); Zhang and Lerman (2014); Li and Haupt (2014); Goes et al. (2014); Lerman and Zhang (2011, 2014); Lerman et al. (2015); Lerman and Maunu (2014); Zhang (2016). Algorithms for robust PCA typically do not perform well in the RSR setting, and algorithms for RSR do not perform well in the robust PCA setting.

Like PCA, RSR is inherently non-convex, due to the non-convexity of $G(D, d)$. Many of the mentioned works have focused on convex relaxations of the non-convex problem (McCoy and Tropp, 2011; Xu et al., 2012; Zhang and Lerman, 2014; Lerman et al., 2015). However, these methods are generally slow and may poorly approximate the underlying non-convex

problem in specific instances. In many practical settings, spherizing the data is a cost effective technique to make PCA more robust (Maronna, 2005; Maronna et al., 2006). This deals with PCA’s sensitivity to the scaling of the data and makes it easier to find directions which robustly capture variance. However, it is still not able to deal with correlated outlier directions and does not have good asymptotic guarantees even for simple models (Lerman and Maunu, 2014).

The works of Lerman and Zhang (2011, 2014) established under a certain model that an underlying subspace is recoverable by the minimization specified in (1). However, they did not provide an algorithm for minimizing this energy. While they consider a more adversarial model, the estimates of these works do not hold for small sample sizes: they only hold for large N . In contrast, our work gives probabilistic exact recovery for finite sample sizes. Lerman and Maunu (2014) proposed an algorithm that aims to solve the non-convex problem, but only obtained theoretical guarantees of approximate recovery for a given model of data, with relatively large samples.

This paper also fits in to the surge of recent work which has focused on non-convex optimization for many structured data problems (Dauphin et al., 2014; Hardt, 2014; Jain et al., 2014; Ge et al., 2015; Lee et al., 2016; Arora et al., 2015; Mei et al., 2016; Ge et al., 2016; Boumal, 2016; Sun et al., 2015b,a). Some work has focused on non-convex optimization for robust PCA (Netrapalli et al., 2014; Yi et al., 2016), which is a related but different problem than RSR. Others have attempted to solve non-convex versions of the RSR problem (Lerman and Maunu, 2014), but don’t have deterministic conditions for recovery.

This work is partially built on optimization on manifolds, and in particular there are important results on optimization over the Grassmannian manifold (Edelman et al., 1999; Absil et al., 2004). Edelman et al. (1999) develop gradient descent on the Grassmannian and give formulations for Newton’s method and conjugate gradient for the Grassmannian. Many other recent works have also focused on optimization on the Grassmannian (Zhang et al., 2009; Goes et al., 2014; Thomas et al., 2014; Zhang and Balzano, 2016; Ye and Lim, 2016; Lim et al., 2016). The work of Zhang and Balzano (2016) examines a rank one geodesic gradient scheme for solving online PCA. Their setting is distinctly different from ours since they attempt to solve the PCA problem rather than RSR. However, they are only able to prove recovery of the PCA solution for a specific model of Gaussian noise, and no generic condition for global recovery is given. Further, while we assume centered data in this paper, Thomas et al. (2014) and Lim et al. (2016) consider estimation on the affine Grassmannian.

3. Outline and Notation

We briefly summarize the results of this paper. In §4, we describe a generic condition which ensures that the energy landscape of (1) behaves nicely around an underlying subspace. We further prove that a geodesic gradient descent method on the Grassmannian can locally recover an underlying subspace for datasets satisfying this condition. Then, §5 shows that the condition holds for a certain model of probabilistic data. Finally, §6 gives simulations which agree with the theoretical results of this paper.

The letter L will be used to refer to linear subspaces. Bold upper case letters are matrices, and bold lower case letters are column vectors. For a matrix \mathbf{A} , $\sigma_j(\mathbf{A})$ will denote the j th singular value of \mathbf{A} , and if \mathbf{A} is square, then $\lambda_j(\mathbf{A})$ will denote the j th eigenvalue. $\text{Sp}(\mathbf{A})$ is the subspace spanned by the columns of \mathbf{A} . For $d \leq D$, the set of orthogonal $D \times d$ matrices is denoted by $O(D, d) = \{\mathbf{V} \in \mathbb{R}^{D \times d} : \mathbf{V}^T \mathbf{V} = \mathbf{I}_d\}$. If $\mathbf{V} \in O(D, d)$, we denote its columns by $(\mathbf{v}_1, \dots, \mathbf{v}_d)$, and may write $\mathbf{V} = (\mathbf{v}_j)_{j=1}^d$. The orthogonal projection matrix onto a subspace $L = \text{Sp}(\mathbf{V})$ is denoted by \mathbf{P}_L , and we will interchangeably use $\mathbf{P}_{\mathbf{V}} = \mathbf{P}_L$. The projection onto the orthogonal complement of L is $\mathbf{Q}_L = \mathbf{I} - \mathbf{P}_L$. The Euclidean 2-norm will be denoted as $\|\cdot\|$. We will denote the largest principal angle between two subspaces using the function $\Theta_1 : G(D, d) \times G(D, d) \rightarrow [0, \pi/2]$. This is defined in the following way: for $\mathbf{V}_1, \mathbf{V}_2 \in O(D, d)$, $\text{Sp}(\mathbf{V}_1) = L_1$, $\text{Sp}(\mathbf{V}_2) = L_2$, we have $\Theta_1(L_1, L_2) = \arccos(\sigma_d(\mathbf{V}_1^T \mathbf{V}_2))$. For a matrix $\mathbf{V} \in O(D, d)$, we will also use the shorthand $\Theta_1(\mathbf{V}, L) = \Theta_1(\text{Sp}(\mathbf{V}), L)$. Finally, for a vector \mathbf{x} and a subspace L , $\angle(\mathbf{x}, L) = \arccos(\|\mathbf{P}_L \mathbf{x}\| / \|\mathbf{x}\|)$ is the angle between \mathbf{x} and L .

4. A Well-Tempered Landscape

Suppose that we are given a dataset partitioned into a subset of inliers lying on (or around) a low-dimensional linear subspace $L^* \in G(D, d)$ and a subset of outliers, whose support set is complementary to that of the inliers. The problem of RSR is to recover the low-dimensional subspace L^* . In order for this problem to be well-defined, basic assumptions must be made. Indeed, if all inliers lie at the origin, then any subspace would be a solution to the RSR problem. Our theoretical results for recovery will depend on a condition formulated later in this section that ensures the problem is well-defined.

First, we lay out some preliminary concepts for optimization over $G(D, d)$ in §4.1. Then, §4.2 discusses some statistics which play a fundamental role in our analysis. Next, §4.3 uses these statistics to develop the generic condition that ensures the energy landscape of (1) behaves nicely. Then, we present a geodesic gradient descent method in §4.4 and show that it is able to recover the underlying subspace with this condition.

4.1 Optimization over $G(D, d)$

The minimization in (1) involves optimization over the Grassmannian manifold. To understand the energy landscape, one must have a basic understanding of the geometry of $G(D, d)$ and how to calculate derivatives over it. We can write the cost function in (1) in two equivalent ways. First, as a function over $G(D, d)$, we write

$$F(L; \mathcal{X}) = \sum_{\mathcal{X}} \|\mathbf{Q}_L \mathbf{x}_i\|. \quad (2)$$

On the other hand, we can represent points in $G(D, d)$ by equivalence classes of points in $O(D, d)$. For any $\mathbf{V} \in O(D, d)$, the subspace $\text{Sp}(\mathbf{V})$ can be represented by the equivalence class $[\mathbf{V}] = \{\mathbf{V}\mathbf{R} : \mathbf{R} \in O(d, d)\}$. For $\mathbf{V} \in O(D, d)$, the cost (2) is equivalent to

$$F(\mathbf{V}; \mathcal{X}) = \sum_{i=1}^N \|\mathbf{I} - \mathbf{V}\mathbf{V}^T\| \mathbf{x}_i. \quad (3)$$

While both formulations are equivalent, (2) is used to formulate geodesic derivatives over $G(D, d)$, while (3) is used to calculate gradients.

One can measure the distance between subspaces in $G(D, d)$ using the principal angles. For a discussion of principal angles, see Appendix A. Denoting the largest principal angle between L_1 and L_2 by $\Theta_1(L_1, L_2)$, we can define a metric on $G(D, d)$ by $\text{dist}(L_1, L_2) = \sin(\Theta_1(L_1, L_2))$. We then define a ball on the metric space $G(D, d)$ by

$$B(L^*, \sin(\gamma)) = \{L \in G(D, d) : \sin(\Theta_1(L, L^*)) \leq \sin(\gamma), j = 1, \dots, d\}.$$

We will interchangeably use $B(L^*, \sin(\gamma))$ to be a subset of $G(D, d)$ and a subset of $O(D, d)$, where each element of $O(D, d)$ gives a (non-unique) orthogonal basis for a subspace.

In the following, we frequently use a construction for geodesics on the Grassmannian. For a review of this construction, see Appendix A or §3.2.1 in Lerman and Zhang (2014). Suppose that the interaction dimension between L_1 and L_2 is k . Let $\theta_1, \dots, \theta_k$ be the principal angles for L_1 and L_2 (in decreasing order), and let the respective principal vectors for L_1 and L_2 be $\mathbf{v}_1, \dots, \mathbf{v}_k$ and $\mathbf{y}_1, \dots, \mathbf{y}_k$. Finally, let $\mathbf{u}_1, \dots, \mathbf{u}_k$ be a complementary orthogonal basis for L_2 with respect to L_1 . We can use these to parametrize a geodesic $L(t)$ with $L(0) = L_1$ and $L(1) = L_2$, the formula of which can be seen in (26). Then, following Lerman and Zhang (2014) and Lerman and Maunu (2014), we can calculate the directional geodesic subderivative of (2) at L_1 in the direction of L_2 :

$$\left. \frac{d}{dt} F(L(t); \mathcal{X}) \right|_{t=0} = - \sum_{\|\mathbf{Q}_L \mathbf{x}_i\| > 0} \frac{\sum_{j=1}^k \theta_j (\mathbf{v}_j^T \mathbf{x}_i) (\mathbf{u}_j^T \mathbf{x}_i)}{\|\mathbf{Q}_L \mathbf{x}_i\|}. \quad (4)$$

A subderivative of (3) with respect to \mathbf{V} is

$$\frac{\partial}{\partial \mathbf{V}} F(\mathbf{V}; \mathcal{X}) = - \sum_{\|\mathbf{Q}_V \mathbf{x}_i\| > 0} \frac{\mathbf{x}_i \mathbf{x}_i^T \mathbf{V}}{\|\mathbf{Q}_V \mathbf{x}_i\|}. \quad (5)$$

Notice that in both of the derivatives (4) and (5), the sum is taken over all points which do not lie in $\text{Sp}(\mathbf{V})$, which makes them both subderivatives. First, for (4), a subderivative of $F(L(t); \mathcal{X})$ at $t = 0$ is any element of the subdifferential at $L(0)$. The subdifferential is the set of all numbers between

$$a = \lim_{t \rightarrow 0^-} \frac{F(L(t); \mathcal{X}) - F(L(0); \mathcal{X})}{t}, \quad b = \lim_{t \rightarrow 0^+} \frac{F(L(t); \mathcal{X}) - F(L(0); \mathcal{X})}{t}.$$

If $a \leq b$, then the subdifferential is $[a, b]$, and, on the other hand, if $a > b$, then the subdifferential is $[b, a]$. For the other case of (5), for any component of \mathbf{V} , \mathbf{V}_{ij} , let Δ be the matrix of all zeros except $\Delta_{ij} = 1$. Then, the subdifferential of $F(\mathbf{V}; \mathcal{X})$ for \mathbf{V}_{ij} is all numbers between

$$a_{ij} = \lim_{t \rightarrow 0^-} \frac{F(\mathbf{V} + t\Delta; \mathcal{X}) - F(\mathbf{V}; \mathcal{X})}{t}, \quad b_{ij} = \lim_{t \rightarrow 0^+} \frac{F(\mathbf{V} + t\Delta; \mathcal{X}) - F(\mathbf{V}; \mathcal{X})}{t}.$$

In future sections, to save space, we will write the sums in (4) and (5) as $\sum_{\mathcal{X}}$ and leave the condition $\|\mathbf{Q}_V \mathbf{x}_i\| > 0$ as implied. Following Section 2.5.3 of Edelman et al. (1999), to respect the geometry of the Grassmannian, the (sub)gradient of (3) is defined as

$$\nabla F(\mathbf{V}; \mathcal{X}) = \mathbf{Q}_V \frac{\partial}{\partial \mathbf{V}} F(\mathbf{V}; \mathcal{X}). \quad (6)$$

4.2 Landscape Statistics

In this section, we define statistics which are inspired by Lerman et al. (2015). These are later used to describe the behavior of the energy landscape around an underlying subspace. We start with more rigorous setting of inliers and outliers. We assume a dataset $\mathcal{X} = \{\mathbf{x}_1, \dots, \mathbf{x}_N\} \subset \mathbb{R}^D$. For the noiseless case, we suppose further that a subset of the points, $\mathcal{X}_1 \subset \mathcal{X}$, lie on a low-dimensional linear subspace $L^* \in G(D, d)$, and the rest of the points, $\mathcal{X}_0 = \mathcal{X} \setminus \mathcal{X}_1$, are in $\mathbb{R}^D \setminus \{L^*\}$. We call \mathcal{X} defined in this way an inliers-outliers dataset. Similarly, a noisy setting occurs when the inliers \mathcal{X}_1 lie near the low-dimensional subspace L^* . Our mathematical analysis requires the following restricted notion, which we refer to as noisy inliers-outliers dataset. Assume an unknown noise parameter $0 < \eta^* < \pi/2$, where often $\eta^* \ll \pi/2$, and define $\mathcal{X}_1 \equiv \mathcal{X}_1(L^*, \eta^*) = \{\mathbf{x}_i \in \mathcal{X} : \angle(\mathbf{x}_i, L^*) \leq \eta^*\}$ and $\mathcal{X}_0 = \mathcal{X}_0(L^*, \eta^*) = \{\mathbf{x}_i \in \mathcal{X} : \angle(\mathbf{x}_i, L^*) > \eta^*\}$. Notice that the points $\mathcal{X}_1(L^*, \eta^*)$ lie in a cone around the subspace L^* . The following statistics are used to further restrict both the noiseless and noisy inliers-outliers model.

The permeance of the inlier dataset \mathcal{X}_1 with respect to the underlying subspace L^* is defined as

$$\mathcal{P}(\mathcal{X}_1, L^*) = \lambda_d \left(\sum_{\mathcal{X}_1} \frac{\mathbf{P}_{L^*} \mathbf{x}_i \mathbf{x}_i^T \mathbf{P}_{L^*}}{\|\mathbf{P}_{L^*} \mathbf{x}_i\|} \right). \quad (7)$$

Here, $\lambda_d(\cdot)$ denotes the d th eigenvalue of a matrix. Notice that the permeance is with respect to a subspace L^* . Large values of \mathcal{P} ensure that the inliers are well-distributed with respect to the underlying subspace. Notice that this is also the d th singular value of the dataset formed by dividing each projected inlier point, $\mathbf{P}_{L^*} \mathbf{x}_i$, by the square root of its norm. In the noiseless case, one can ignore the projections \mathbf{P}_{L^*} since they are the identity on L^* .

We define the alignment statistic of the outlier dataset \mathcal{X}_0 with respect to a subspace $\text{Sp}(\mathbf{V})$ as

$$\mathcal{A}(\mathcal{X}_0, \mathbf{V}) = \mathcal{A}(\mathcal{X}_0, \text{Sp}(\mathbf{V})) = \sigma_1(\nabla F(\mathbf{V}; \mathcal{X}_0)). \quad (8)$$

In (8), $\sigma_1(\cdot)$ denotes the largest singular value of a matrix. In effect, if this term is always small, then the outliers are not concentrated in a certain d -dimensional space. In our later analysis, we will use a simple bound for \mathcal{A} :

$$\mathcal{A}(\mathcal{X}_0, \mathbf{V}) \leq \sqrt{N_{\text{out}}} \|\mathbf{X}_0\|_2. \quad (9)$$

Here, \mathbf{X}_0 is the matrix formed by the outlier data points. The derivation for this bound is left to Appendix E. While convenient, we note that this bound is not tight.

The final statistic we define is the stability statistic. Then, using the permeance and alignment defined in (7) and (8), the stability statistic is

$$\mathcal{S}(\gamma, \eta, L^*) = \cos(\gamma + \eta) \cos(\eta) \mathcal{P}(\mathcal{X}_1(L^*, \eta), L^*) - \max_{\mathbf{V} \in B(L^*, \sin(\gamma)) \setminus B(L^*, \sin(\eta))} \mathcal{A}(\mathcal{X}_0(L^*, \eta), \mathbf{V}). \quad (10)$$

The noiseless stability statistic is given by $\mathcal{S}(\gamma, 0, L^*)$. Note that $\mathcal{S}(0, 0, L^*) = \mathcal{P}(\mathcal{X}_1, L^*) - \mathcal{A}(\mathcal{X}_0, L^*)$ is a tighter stability condition than the one in Lerman et al. (2015). However, as γ increases, \mathcal{S} decreases and our estimate suffers.

4.3 The Local Landscape under Stability

We will show that positivity of the stability statistic given in (10) implies that L^* is a stable critical point for the optimization in (1). We first consider the noiseless case and set $\eta = 0$ in $\mathcal{S}(\gamma, \eta, L^*)$ and then generalize it to the noisy setting. The following theorem gives a characterization of the energy landscape of (2) in $\overline{B(L^*, \sin(\gamma))} \subset G(D, d)$.

Theorem 1 (Stability of L^*) *Suppose that an inliers-outliers dataset with an underlying subspace L^* satisfies $\mathcal{S}(\gamma, 0, L^*) > 0$, for some $0 < \gamma < \pi/2$. Then, all points in $\overline{B(L^*, \sin(\gamma))} \setminus \{L^*\}$ have a directional subdifferential strictly less than $-\mathcal{S}(\gamma, 0, L^*)$, that is, it is a direction of decreasing cost. This implies L^* is the only local minimizer in $\overline{B(L^*, \sin(\gamma))}$.*

Proof

We will show that, for any $L \in \overline{B(L^*, \sin(\gamma))} \setminus \{L^*\}$, there is a geodesic $L(t)$ with $L(0) = L$ and an open interval $(0, \delta(L))$ such that

$$F(L(t); \mathcal{X}) < F(L; \mathcal{X}) \text{ and } \Theta_1(L(t), L^*) < \Theta_1(L, L^*), \forall t \in (0, \delta(L)). \quad (11)$$

We will then show that (11) implies that L^* is a local minimizer by a perturbation argument.

Fix a subspace $L \in \overline{B(L^*, \sin(\gamma))} \setminus \{L^*\}$, and let the principal angles between L and L^* be $\theta_1, \dots, \theta_d$. Also, choose a set of corresponding principal vectors $\mathbf{v}_1, \dots, \mathbf{v}_d$ and $\mathbf{y}_1, \dots, \mathbf{y}_d$, and let l be the maximum index such that $\theta_1 = \dots = \theta_l$. We let $\mathbf{u}_1, \dots, \mathbf{u}_l$ be complementary orthogonal vectors for $\mathbf{v}_1, \dots, \mathbf{v}_l$ and $\mathbf{y}_1, \dots, \mathbf{y}_l$, which exist since $\Theta_1(L, L^*) > 0$. Parametrize the particular geodesic

$$L(t) = \text{Sp}(\mathbf{v}_1 \cos(t) + \mathbf{u}_1 \sin(t), \dots, \mathbf{v}_l \cos(t) + \mathbf{u}_l \sin(t), \mathbf{v}_{l+1}, \dots, \mathbf{v}_d).$$

This geodesic moves only the furthest directions of $L(0)$ towards L^* , and we have removed dependence on θ_1 , since this unnecessarily impacts the magnitude of the geodesic derivative (4). Then, following (4), we have

$$\begin{aligned} \left. \frac{d}{dt} F(L(t); \mathcal{X}) \right|_{t=0} &= - \sum_{j=1}^l \sum_{\mathcal{X}} \frac{\mathbf{v}_j^T \mathbf{x}_i \mathbf{x}_i^T \mathbf{u}_j}{\|\mathbf{Q}_L \mathbf{x}_i\|} \\ &= - \sum_{j=1}^l \left(\sum_{\mathcal{X}_1} \frac{\mathbf{v}_j^T \mathbf{x}_i \mathbf{x}_i^T \mathbf{u}_j}{\|\mathbf{Q}_L \mathbf{x}_i\|} + \sum_{\mathcal{X}_0} \frac{\mathbf{v}_j^T \mathbf{x}_i \mathbf{x}_i^T \mathbf{u}_j}{\|\mathbf{Q}_L \mathbf{x}_i\|} \right) \\ &\leq - \sum_{j=1}^l \left(\frac{\cos(\theta_1) \sin(\theta_1)}{\sin(\theta_1)} \sum_{\mathcal{X}_1} \frac{\mathbf{y}_j^T \mathbf{x}_i \mathbf{x}_i^T \mathbf{y}_j}{\|\mathbf{x}_i\|} - \max_{\mathbf{V} \in \overline{B(L^*, \sin(\gamma))}} \sigma_1(\nabla F(\mathbf{V}; \mathcal{X}_0)) \right) \\ &\leq -l\mathcal{S}(\gamma, 0, L^*) < -\mathcal{S}(\gamma, 0, L^*) < 0. \end{aligned} \quad (12)$$

Thus, (12) implies that every subspace in $\overline{B(L^*, \sin(\gamma))} \setminus \{L^*\}$ has a direction with negative local subderivative.

If $l < d$, then let $\delta(L) = \theta_l - \theta_{l+1}$, and otherwise let $\delta(L) = \theta_l$. Then, notice that for all $L(\tilde{t})$, $\tilde{t} \in (-\pi/2 + \gamma, \delta(L))$, we have the same bound

$$\left. \frac{d}{dt} F(L(t); \mathcal{X}) \right|_{t=\tilde{t}} < -\mathcal{S}(\gamma, 0, L^*) < 0.$$

This means that at $L(0)$, the subdifferential is bounded above by $-\mathcal{S}(\gamma, 0, L^*)$. This follows from the fact that the one-dimensional continuous function $F(L(t); \mathcal{X})$ has subdifferential at $L(0)$ bounded by the maximum subderivatives of $F(L(t); \mathcal{X})$ as $t \rightarrow 0^\pm$. Thus, we have proven (11), since $F(L(t); \mathcal{X})$ must be decreasing on $(0, \delta(L))$.

To show that (11) implies that L^* is a local minimizer, consider a one-dimensional perturbation of L^* , L' . In other words, $\Theta_1(L^*, L') > 0$ and $\Theta_2(L^*, L') = 0$. Then, (11) implies that if $L(t)$ is the geodesic between L' and L^* , then $F(L(t); \mathcal{X})$ is decreasing for $t \in (0, \Theta_1(L', L^*))$. The more general perturbation case is just an extension of this argument. Indeed a d -dimensional perturbation may be written as a sequence of 1-dimensional perturbations. ■

The following theorem generalizes Theorem 1 for the case of a noisy inliers-outliers dataset. The proof of this theorem is left to Appendix B.

Theorem 2 (Stability of $B(L^*, \sin(\eta))$ Under Noisy) *Suppose that a noisy inliers-outliers dataset with an underlying subspace L^* satisfies $\mathcal{S}(\gamma, \eta, L^*) > 0$, for some $0 < \eta < \gamma < \pi/2$. Then, all points in $\overline{B(L^*, \sin(\gamma))} \setminus B(L^*, \sin(\eta))$ have a directional subdifferential strictly less than $-\mathcal{S}(\gamma, \eta, L^*)$, that is, it is a direction of decreasing cost. This implies that the only local minimizers and saddle points in $\overline{B(L^*, \sin(\gamma))}$ are in $B(L^*, \sin(\eta))$.*

4.4 A Geodesic Gradient Method

We will use gradient descent to find directions which span the underlying subspace L^* . Denoting the singular value decomposition $-\nabla F(\mathbf{V}; \mathcal{X}) = \mathbf{U}\Sigma\mathbf{W}^T$, Theorem 2.3 of Edelman et al. (1999) states that the geodesic starting at $\mathbf{V}(0) = \mathbf{V}$ with $\dot{\mathbf{V}}(0) = -\nabla F(\mathbf{V}; \mathcal{X})$ is

$$\mathbf{V}(t) = \mathbf{V}\mathbf{W} \cos(\Sigma t)\mathbf{W}^T + \mathbf{U} \sin(\Sigma t)\mathbf{W}^T. \quad (13)$$

Here, \sin and \cos are the typical matrix \sin and \cos .

We can now construct a geodesic gradient method. At a point \mathbf{V}^k , we may choose a value of t and step along the geodesic defined in (13) to the next iterate. For a choice of t^k , the sequence generated in this way has the form $\mathbf{V}^{k+1} = \mathbf{V}^k(t^k)$. For ease of analysis, we consider the step size rule $t^k = s/\sqrt{k}$ for some initial step size s . In practice, we advocate using line search to select an appropriate step size since it seems to have faster convergence. The full algorithm is given in Algorithm 1. The complexity of this algorithm is $O(TNDd)$, where T is the number of iterations. Empirically, with nice enough data, we have observed linear convergence with line search, so T is generally small. We compare the rate of convergence for s/\sqrt{k} and line search step size later in Figure 4. In the remainder of this paper, we will refer to Algorithm 1 as GGD.

Algorithm 1 RSR by Geodesic Gradient Descent

- 1: Input: dataset \mathcal{X} , subspace dimension d , initial step size s , tolerance τ
 - 2: Output: $\mathbf{V}^* \in O(D, d)$, whose columns span the robust subspace
 - 3: $\mathbf{V}^1 = PCA(\mathbf{X}, d)$
 - 4: $k = 1$
 - 5: **while** $\Theta_1(\mathbf{V}^k, \mathbf{V}^{k-1}) > \tau$ or $k = 1$ **do**
 - 6: $\mathbf{U}^k \boldsymbol{\Sigma}^k \mathbf{W}^k = -\nabla F(\mathbf{V}^k; \mathcal{X})$
 - 7: $t^k = s/\sqrt{k}$
 - 8: $\mathbf{V}^{k+1} = \mathbf{V}^k \mathbf{W}^k \cos(\boldsymbol{\Sigma}^k t^k) \mathbf{W}^{kT} + \mathbf{U}^k \sin(\boldsymbol{\Sigma}^k t^k) \mathbf{W}^{kT}$ $\triangleright (13)$
 - 9: $k = k + 1$
 - 10: **end while**
-

Theorem 1 implies that if $\mathcal{S}(\gamma, 0, L^*) > 0$, then L^* is the only limit point in $\overline{B(L^*, \sin(\gamma))}$ for the GGD. In other words, there is no need to worry about saddle points or non-optimal critical points in this set. This result is more precisely stated in the following theorem. The proof of this theorem is left to Appendix C.

Theorem 3 (Noiseless local convergence) *Assume an inliers-outliers dataset with an underlying subspace L^* . Suppose that there exists $0 < \gamma < \pi/2$ such that $\mathcal{S}(\gamma, 0, L^*) > 0$, and suppose that the initial GGD iterate is $\mathbf{V}^1 \in \overline{B(L^*, \sin(\gamma))}$. Then, for sufficiently small s as input, GGD converges to L^* with rate $\Theta_1(L_k, L^*) < O(1/\sqrt{k})$.*

The next theorem shows that for noisy inliers-outliers dataset with underlying subspace L^* , $\mathcal{S}(\gamma, \eta, L^*) > 0$ implies that \mathbf{V}^k converges to $\overline{B(L^*, \sin(\eta))}$ in $\overline{B(L^*, \sin(\gamma))}$. The proof is deferred until Appendix D.

Theorem 4 (Noisy local convergence) *Assume a noisy inliers-outliers dataset with an underlying subspace L^* . Suppose that there exist numbers $0 < \eta < \gamma < \pi/2$ such that $\mathcal{S}(\gamma, \eta, L^*) > 0$, and suppose that the initial GGD iterate is $\mathbf{V}^1 \in \overline{B(L^*, \sin(\gamma))}$. Then, for sufficiently small s as input, GGD converges to $\overline{B(L^*, \sin(\eta))}$ with rate $O(1/\sqrt{k})$.*

5. Guarantees of Stability for Special Data Models

Here we examine a data model under which $\mathcal{S}(\gamma, \eta, L^*) > 0$. In §5.1 we show that the condition holds for a simple inlier-outlier mixture of Gaussians, referred to as the Generalized Haystack Model. We also extend the result to the case of noisy inliers. Then, §5.2 offers some discussion of the results and compares with other works on RSR.

5.1 Recovery Guarantees under the Generalized Haystack Model

In this section, we prove that under a certain model of data, $\mathcal{S}(\gamma, \eta, L^*) > 0$ with high probability. The model is a generalization of the Haystack Model of Lerman et al. (2015). Fix a positive diagonal matrix $\mathbf{\Lambda}_{\text{in}} \in \mathbb{R}^{d \times d}$ and $\mathbf{V}^* \in O(D, d)$, which spans $L^* \in G(D, d)$. Letting $\boldsymbol{\Sigma}_{\text{in}} = \mathbf{V}^* \mathbf{\Lambda}_{\text{in}} \mathbf{V}^{*T}$, we assume that N_{in} inliers are distributed i.i.d. $\mathcal{N}(0, \boldsymbol{\Sigma}_{\text{in}}/d)$. Fix a symmetric positive semidefinite matrix $\boldsymbol{\Sigma}_{\text{out}} \in \mathbb{R}^{D \times D}$ and assume N_{out} outliers are distributed i.i.d. $\mathcal{N}(0, \boldsymbol{\Sigma}_{\text{out}}/D_{\text{out}})$, where D_{out} is the rank of $\boldsymbol{\Sigma}_{\text{out}}$. This specifies a Generalized Haystack Model with parameters $N_{\text{in}}, \boldsymbol{\Sigma}_{\text{in}}, N_{\text{out}}, \boldsymbol{\Sigma}_{\text{out}}, D$, and d .

Under conditions on these parameters, we will show it is possible to exactly recover the underlying subspace, L^* . Scaling the inlier and outlier covariance matrices by d and D_{out} , respectively, ensures that in the uniform case (where Σ_{in} and Σ_{out} are orthogonal projections onto subspaces of \mathbb{R}^D of dimensions d and D_{out} respectively) the inliers and outliers have the same typical length. Thus, with this normalization, differences in the traces of Σ_{in} and Σ_{out} translate into differences in typical scale between inliers and outliers. It is also important to prove results for general Gaussian distributions rather than just spherically symmetric Gaussians (like in the Haystack Model), because simpler strategies, like PCA outlier filtering, can be applied to the symmetric case. The Generalized Haystack Model allows for certain adversarial outliers: for example, outliers can be in a low-dimensional subspace as well.

Theorem 5 (Stability of the Generalized Haystack Model) *Suppose that the dataset \mathcal{X} follows the Generalized Haystack Model with parameters N_{in} , Σ_{in} , N_{out} , Σ_{out} , D , and d . Suppose that, for some absolute constant C_1 , and other constants $0 < \gamma < \pi/2$, $0 < a < 1$, and $C_0 > 0$,*

$$\cos(\gamma)\lambda_d(\Sigma_{\text{in}}^{1/2}) \left((1-a)\sqrt{\frac{N_{\text{in}}}{d}} - C_1 \right)^2 > \lambda_1(\Sigma_{\text{out}}^{1/2}) \left[\frac{N_{\text{out}}}{\sqrt{dD_{\text{out}}}} + \sqrt{\frac{N_{\text{out}}}{d}} + \sqrt{\frac{2N_{\text{out}}C_0}{dD_{\text{out}}}} \right], \quad (14)$$

$$N_{\text{in}} > \frac{C_1^2}{(1-a)^2} d. \quad (15)$$

Then $\mathcal{S}(\gamma, 0, L^*) > 0$ with probability at least $1 - 2e^{-c_1 a^2 N_{\text{in}}} - e^{-C_0}$, for some absolute constant c_1 .

Proof For the outliers, we have the simple bound from (9). Noting that

$$\|\mathbf{X}_0\|_2 = \|\Sigma_{\text{out}}^{1/2} \Sigma_{\text{out}}^{-1/2} \mathbf{X}_0\|_2 \leq \|\Sigma_{\text{out}}^{1/2}\|_2 \|\Sigma_{\text{out}}^{-1/2} \mathbf{X}_0\|_2,$$

we can again apply Proposition B.3 of Lerman et al. (2015) since $\Sigma_{\text{out}}^{-1/2} \mathbf{X}_0$ is isometric. Thus, we have the bound

$$\sqrt{N_{\text{out}}}\|\mathbf{X}_0\|_2 \leq \left\| \Sigma_{\text{out}}^{1/2} \right\|_2 \sqrt{N_{\text{out}}} \left[\sqrt{\frac{N_{\text{out}}}{D_{\text{out}}}} + 1 + \sqrt{\frac{2C_0}{D_{\text{out}}}} \right], \text{ w.p. at least } 1 - e^{-C_0}. \quad (16)$$

For the inliers, we need to bound $\mathcal{P}(\mathcal{X}_1, L^*)$. Notice that

$$\frac{\lambda_d(\Sigma_{\text{in}}^{1/2})}{2} \leq E_{\mathcal{N}(0, \Sigma_{\text{in}}/d)}(\mathbf{x}^T \mathbf{x} / \|\mathbf{x}\|) = E_{\mathcal{N}(0, \Sigma_{\text{in}}(d+1)/d^2)}(\|\mathbf{x}\|) \leq \lambda_1(\Sigma_{\text{in}}^{1/2}).$$

Using Theorem 5.39 in Vershynin (2012b), if $N_{\text{in}} > 2C_1^2 d$,

$$\lambda_d \left(\sum_{\mathcal{X}_1} \frac{\mathbf{x}_i \mathbf{x}_i^T}{\|\mathbf{x}_i\|} \right) > \frac{\lambda_d(\Sigma_{\text{in}}^{1/2})}{\sqrt{d}} \left((1-a)\sqrt{N_{\text{in}}} - C_1 \sqrt{d} \right)^2, \text{ w.p. } 1 - 2e^{-c_1 a^2 N_{\text{in}}}. \quad (17)$$

Here, C_1 and c_1 depend only on $\max_i \|\mathbf{x}_i / \sqrt{\|\mathbf{x}_i\|}\|_{\psi_2} = \|\mathbf{x}_1 / \sqrt{\|\mathbf{x}_1\|}\|_{\psi_2}$, where $\|\cdot\|_{\psi_2}$ is defined in Definition 5.7 of Vershynin (2012b). Thus, these are absolute constants that do not depend on N_{in} , D , or d .

It is left to compare the bounds. Notice that (14) can be obtained by requiring the right hand side of (16) to be less than $\cos(\gamma)$ times the right hand side of (17). Also, (15) must hold in order for us to apply Theorem 5.39 of Vershynin (2012b). Thus, (14) and (15) are sufficient conditions for $\mathcal{S}(\gamma, 0, L^*) > 0$ with probability $1 - 2e^{-c_1 a^2 N_{\text{in}}} - e^{-C_0}$. \blacksquare

In the large sample regime, we have the following extension of Theorem 5 which gives a complete recovery guarantee. For this to hold, notice that there is an additional requirement on the ratio $N_{\text{in}}/N_{\text{out}}$, although it is somewhat weaker than (14) for sufficiently large neighborhoods $\overline{B}(L^*, \sin(\gamma))$. A short proof for this theorem is given in Appendix F.

Theorem 6 (Complete guarantee for the Generalized Haystack Model) *Suppose that the dataset \mathcal{X} follows the Generalized Haystack Model with parameters N_{in} , $\boldsymbol{\Sigma}_{\text{in}}$, N_{out} , $\boldsymbol{\Sigma}_{\text{out}}$, D , and d , and (14) and (15) are satisfied for some $0 < \gamma < \pi/2$. Suppose also that*

$$\frac{N_{\text{in}}}{N_{\text{out}}} > \frac{\sqrt{2}}{\sin(\gamma)} \frac{d}{D_{\text{out}}} \frac{\lambda_1(\boldsymbol{\Sigma}_{\text{out}})}{\lambda_d(\boldsymbol{\Sigma}_{\text{in}})}. \quad (18)$$

Then, for large enough $N = N_{\text{out}} + N_{\text{in}}$, Algorithm 1 recovers L^ with high probability.*

The result of Theorem 5 is stable to noise as well. In this case, we slightly modify the Haystack Model with parameters N_{in} , $\boldsymbol{\Sigma}_{\text{in}}$, N_{out} , $\boldsymbol{\Sigma}_{\text{out}}$, D , and d . We remind the reader that under the Generalized Haystack Model, the inliers are distributed i.i.d. $N(0, \boldsymbol{\Sigma}_{\text{in}}/d)$ and outliers are distributed i.i.d. $N(0, \boldsymbol{\Sigma}_{\text{out}}/D_{\text{out}})$. The Noisy Generalized Haystack Model is a Generalized Haystack Model, but with perturbed inliers as follows. Given the set of inliers $\{\mathbf{x}_i^{L^*}\}_{i=1}^{N_{\text{in}}}$ generated by the Generalized Haystack Model, the inliers $\{\mathbf{x}_i\}_{i=1}^{N_{\text{in}}}$ of the generalized noisy model are generated by $\mathbf{x}_i = \mathbf{x}_i^{L^*} + \boldsymbol{\epsilon}_i$, where $\boldsymbol{\epsilon}_i$ are i.i.d. with $\boldsymbol{\epsilon}_i | \mathbf{x}_i^{L^*} \sim \mathcal{N}(0, \|\mathbf{x}_i^{L^*}\|^2 \sigma_{\text{noise}}^2 \mathbf{Q}_{L^*} / (D - d))$. Notice that the variance is dependent on the norm of the projection on the subspace, which causes inliers to lie inside of a small cone around the subspace with high probability. A comparison of the Haystack and Noisy Haystack Model is displayed in Figure 2. More than 95% of inliers have angle less than $30\sigma_{\text{noise}}$ with L^* . The following theorem proves that $\mathcal{S}(\gamma, \eta, L^*) > 0$ for the Noisy Generalized Haystack Model, under certain extra conditions. The proof of this theorem is left to Appendix G.

Theorem 7 (Stability of the Noisy Generalized Haystack Model) *Let \mathcal{X} be distributed according to the Noisy Haystack Model with parameters N_{in} , $\boldsymbol{\Sigma}_{\text{in}}$, N_{out} , $\boldsymbol{\Sigma}_{\text{out}}$, D , d , and σ_{noise} . Suppose that for some absolute constant C_1 , and fixed constants $0 < a < 1$, $C_0 > 0$, $b > 0$, $\eta = \sigma_{\text{noise}} \sqrt{1 + \sqrt{b} + b}$ and $0 < \eta < \gamma < \pi/2$, (15) holds and*

$$\cos(\gamma + \eta) \cos(\eta) \lambda_d \left(\boldsymbol{\Sigma}_{\text{in}}^{1/2} \right) \left((1 - a) \sqrt{\frac{N_{\text{in}}}{d}} - C_1 \right)^2 > \lambda_1 \left(\boldsymbol{\Sigma}_{\text{out}}^{1/2} \right) \left[\frac{N_{\text{out}}}{\sqrt{d} D_{\text{out}}} + \sqrt{\frac{N_{\text{out}}}{d}} + \sqrt{\frac{2N_{\text{out}} C_0}{d D_{\text{out}}}} \right]. \quad (19)$$

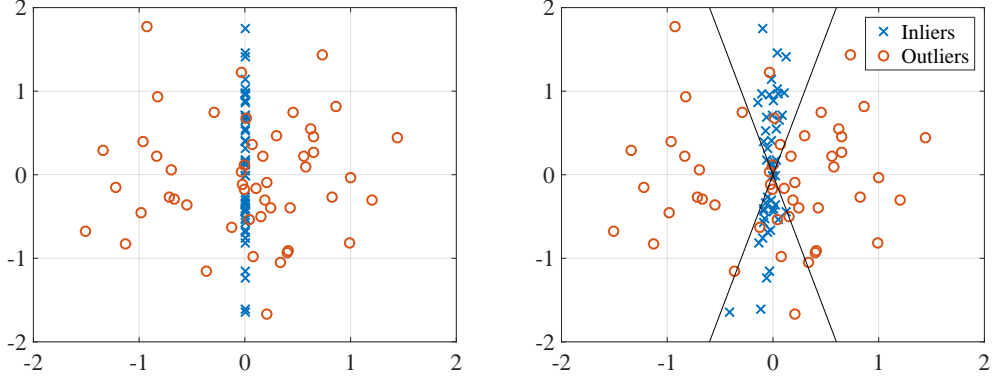


Figure 2: Comparison of the Generalized Haystack Model and Noisy Generalized Haystack Model. In both plots, $N_{\text{in}} = 50$, $\Sigma_{\text{in}} = (0, 1)^T(0, 1)$, $N_{\text{out}} = 50$, $\Sigma_{\text{out}} = \mathbf{I}_2$, $D = 2$, and $d = 1$. Left: Noiseless Haystack Model. Right: Noisy Haystack Model with $\sigma_{\text{noise}}^2 = 10^{-3}$. A cone with angle $30\sigma_{\text{noise}}$ is depicted since most inliers lie within this cone.

Then $\mathcal{S}(\gamma, \eta, L^*) > 0$ with probability at least $1 - 2e^{-c_1 a^2 N_{\text{in}}} - e^{-C_0} - N_{\text{in}} e^{-b(D-d)}$ for some absolute constant c_1 .

As we can see, the noise adds an additional factor to the probability of $N_{\text{in}} e^{-b(D-d)}$, which is small for sufficiently large dimension D and sufficiently small subspace dimension d . As we can see, though, our theory is not able to handle numbers of points that are exponential in relation to the ambient dimension. Also, we note that this result encompasses results for “noisy” outliers as well, since the outlier covariance has arbitrary rank. For example, one can represent noisy outliers around a subspace with $\Sigma_{\text{out}} = \beta \mathbf{P}_L + \tilde{\sigma}_{\text{noise}}^2 \mathbf{Q}_L$, where β determines the scale of the outliers and $\tilde{\sigma}_{\text{noise}}$ determines the scale of the noise.

5.2 Discussion of Theorems

In order to better understand the technical conditions in (14) and (19) we consider the asymptotic case, where $N \rightarrow \infty$. In this case we translate conditions (14) and (19) into lower bounds on the signal-to-noise ratio (SNR), which is the sampling ratio of inliers to outliers. We note that the left hand side of (14) in Theorem 5 is $O(\lambda_d(\Sigma_{\text{in}}^{1/2})N_{\text{in}}/d)$ and the right hand side is $O(\lambda_1(\Sigma_{\text{out}}^{1/2})N_{\text{out}}/\sqrt{dD_{\text{out}}})$. For the full theoretical guarantee, we also need to consider (18). From these equations, for a fixed γ , we conclude that our theoretical asymptotic SNR for the Generalized Haystack Model is

$$\text{SNR} \geq \max \left(\frac{1}{\cos(\gamma)(1-a)^2} \frac{\lambda_1(\Sigma_{\text{out}}^{1/2})}{\lambda_d(\Sigma_{\text{in}}^{1/2})} \sqrt{\frac{d}{D_{\text{out}}}}, \frac{\sqrt{2}}{\sin(\gamma)} \frac{\lambda_1(\Sigma_{\text{out}})}{\lambda_d(\Sigma_{\text{in}})} \frac{d}{D_{\text{out}}} \right). \quad (20)$$

We note that for the noisy case, where (19) replaces (14), the above asymptotic SNR is similar, where $\cos(\gamma)$ is multiplied by $\cos(\gamma + \eta)$.

GGD	$N_{\text{in}}/N_{\text{out}} \geq \max \left(\frac{1}{\cos(\gamma)(1-a)^2} \frac{\sigma_{\text{out}}}{\sigma_{\text{in}}} \sqrt{\frac{d}{D}}, \frac{\sqrt{2}}{\sin(\gamma)} \frac{\sigma_{\text{out}}^2}{\sigma_{\text{in}}^2} \frac{d}{D} \right)$
	<i>Generic condition and result for Generalized Haystack Model.</i>
FMS	$N_{\text{in}}/N_{\text{out}} \approx 0$
	<i>Approximate recovery for large samples from spherized Haystack or from two 1-dimensional subspaces on sphere.</i>
Reaper	$N_{\text{in}}/N_{\text{out}} \geq 16 \frac{\sigma_{\text{out}}}{\sigma_{\text{in}}} \frac{d}{D}$
	<i>Generic condition, but only proven to hold for Haystack and $d < (D - 1)/2$.</i>
GMS	$N_{\text{in}}/N_{\text{out}} \geq 4 \frac{\sigma_{\text{out}}}{\sigma_{\text{in}}} \frac{d}{\sqrt{(D-d)D}}$
	<i>Generic condition, extends to Haystack with asymmetric outliers.</i>
OP/LLD	$N_{\text{in}}/N_{\text{out}} \geq \frac{121d}{9} O(\max(1, \log(N)/d))$
	<i>Generic condition with last term replaced by an inlier incoherence parameter μ.</i>
HR-PCA	$N_{\text{in}}/N_{\text{out}} \rightarrow \infty$
	<i>Weak lower bound on the expressed variance.</i>
TME/(D)RF	$N_{\text{in}}/N_{\text{out}} > \frac{d}{D-d}$
	<i>Result for “general-position” data, but does not extend to noise.</i>

Table 1: Asymptotic SNR’s under the Haystack Model for various theoretically-guaranteed RSR algorithms and summary of guarantees.

We hypothesize that the asymptotic SNR of GGD may be improved by replacing the above factor $\sqrt{d/D_{\text{out}}}$ with $\min(\sqrt{d/D_{\text{out}}}, Cd/(D_{\text{out}} - d))$, where C is an absolute constant, but we have not yet been able to prove it. This hypothesis is based on the fact that for each \mathbf{V} , we can show that $\mathcal{A}(\mathcal{X}_0, \mathbf{V}) \leq O(\lambda_1(\boldsymbol{\Sigma}_{\text{out}}^{1/2})N_{\text{out}}/(D_{\text{out}} - d))$ with high probability, but a covering argument is not simple in this case.

As the SNR grows, we see that larger values of γ may be tolerated for GGD. In particular, for large sample sizes and sufficiently large SNRs, γ can be sufficiently close to $\pi/2$. In this case, random initializations of GGD are expected to work as well as the PCA initialization. We quantify this claim more rigorously in the special case where $D_{\text{out}} = D$, $d < D/2$ and $d, D \rightarrow \infty$. Based on the analysis of extreme singular values of random Gaussian matrices (Rudelson and Vershynin, 2008), it can be shown that with high probability, a random initialization lies in $\overline{B(L^*, \sin(\gamma))} \setminus \{L^*\}$, where $\cos(\gamma) = O(1/\sqrt{Dd})$. Therefore, GGD with random initialization succeeds with high probability under the given assumptions on d and D when $N_{\text{in}}/N_{\text{out}} \geq O\left(\frac{1}{(1-a)^2} \frac{\sigma_{\text{out}}}{\sigma_{\text{in}}} d\right)$.

We note that Theorems 5 and 6 both depend on the inlier and outlier variances. One can alleviate the dependence on these terms by introducing spherization into the GGD procedure. While it is hard to prove that this works for general covariances $\boldsymbol{\Sigma}_{\text{in}}$ and $\boldsymbol{\Sigma}_{\text{out}}$, this at least works when $\boldsymbol{\Sigma}_{\text{in}} = \sigma_{\text{in}}^2 \mathbf{P}_{L^*}$ and $\boldsymbol{\Sigma}_{\text{out}} = \sigma_{\text{out}}^2 \mathbf{I}$. Such a statement would be similar to the statement of Theorem 1 in the earliest arXiv version of Lerman et al. (2015), which is located at <https://arxiv.org/abs/1202.4044v1>.

It is important to compare our results to the theoretical results of other RSR algorithms. Lerman and Maunu (2014) try to solve the same optimization using Iteratively Reweighted Least Squares, but are only able to prove approximate recovery for large sample sizes under the spherized Haystack Model or another special mixture model. This is the only prior non-convex optimization approach to RSR with theoretical guarantees that we are aware of. This work, on the other hand, is able to prove exact recovery for small sample sizes with restrictions on the parameters. The work of Lerman et al. (2015) solves a convex relaxation of the problem (1) and gives strong guarantees on recovery. We find the theory for the geodesic gradient method here has many similarities to theirs, with slightly worse bounds on the parameters in Theorems 5 and 7, but with applicability to a more general model.

At last, we consider all theoretically guaranteed RSR algorithms we are aware of and compare their lowest asymptotic SNRs for the Haystack model. We recall that the Haystack model assumes that $\Sigma_{\text{in}} = \sigma_{\text{in}}^2 \mathbf{P}_{L^*}$ and $\Sigma_{\text{out}} = \sigma_{\text{out}}^2 \mathbf{I}_D$. Table 1 imitates Table 1 of Zhang and Lerman (2014). It compares lower bounds on asymptotic SNR under the Haystack Model and also briefly describes the actual data model that each algorithm has guarantees for. The algorithms include Geodesic gradient descent (GGD), FMS (Lerman and Maunu, 2014), Reaper (Lerman et al., 2015), GMS (Zhang and Lerman, 2014), OP (Xu et al., 2012) and LLD (McCoy and Tropp, 2011), HR-PCA (Xu et al., 2013), Tyler’s M-estimator (TME) (Zhang, 2016), and RF (Hardt and Moitra, 2013).

6. Simulations

This section will first attempt to demonstrate the stability condition \mathcal{S} from (10). While we cannot explicitly evaluate the maximum within this expression, we can instead simulate the values achieved by

$$\cos(\gamma + \eta) \cos(\eta) \mathcal{P}(\mathcal{X}_1, L^*) - \mathcal{A}(\mathcal{X}_0, \mathbf{V}), \quad (21)$$

for \mathbf{V} in a small neighborhood of L^* . To simulate the noiseless case, we set $\eta = 0$ in (21), and for the noisy case we can choose some value of $\eta > 0$.

The values achieved by (21) are simulated in Figure 3 for the noiseless and noisy case. The datasets for these figures are generated according to the Generalized Haystack Model outlined in §5.1, with $\Sigma_{\text{in}} = \mathbf{P}_{L^*}$ and $\Sigma_{\text{out}} = \mathbf{I}$. For this data, we choose a noise level of $\sigma_{\text{noise}}^2 = 10^{-3}$ in the noisy case. For each plot, the y -axis represents a distance from the underlying subspace L^* in terms of the maximum principal angle, and the x -axis represents randomly generated subspaces at that distance from L^* . The color represents the value of (21). As we can see, the value of (21) is indeed positive for large neighborhoods of L^* . In both examples, we choose $\gamma = \pi/4$, the noiseless case takes $\eta = 0$, and we choose $\eta = 2 \arctan(\sigma_{\text{noise}}) \approx 0.06$ for the noisy case. Notice that the dependence on η in the noisy condition makes things slightly weaker than in the noiseless case. Despite this extra dependence on η , the condition still seems to hold in $\overline{B(L^*, \sin(\pi/4))} \setminus B(L^*, \sin(\eta))$.

We also simulate the convergence properties of the GGD method in Figure 4. The data was generated according to the (Generalized) Haystack Model with parameters $N_{\text{in}} = 200$, $\Sigma_{\text{in}} = \mathbf{P}_{L^*}$, $N_{\text{out}} = 200$, $\Sigma_{\text{out}} = \mathbf{I}$, $D = 100$, and $d = 5$. We compare three different choices of step size. The blue line denotes the convergence of the s/\sqrt{k} step size choice in Algorithm 1 with $s = 1/N$. The red line denotes the convergence of line search at each

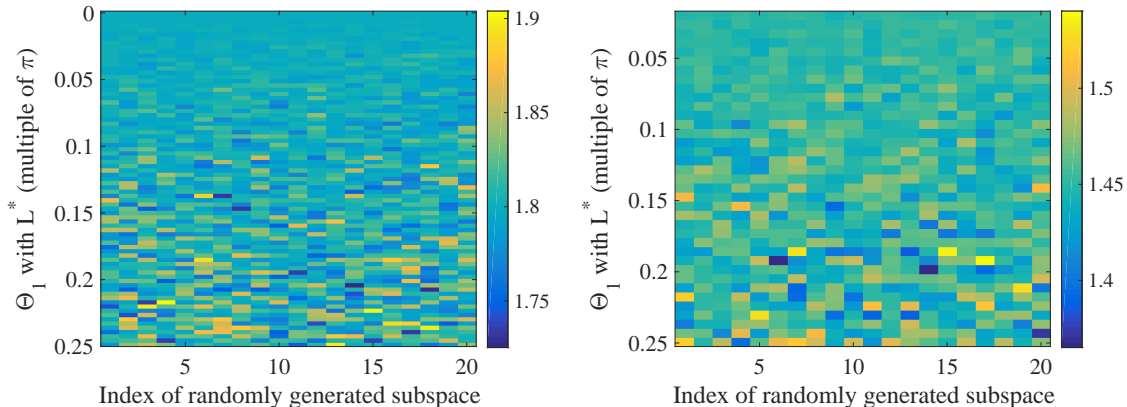


Figure 3: Simulation of the stability statistic. Data was generated for the Generalized Haystack Model with parameters $D = 200$, $d = 10$, $N_{\text{in}} = N_{\text{out}} = 200$, and $\Sigma_{\text{in}} = \mathbf{P}_{L^*}$ and $\Sigma_{\text{out}} = \mathbf{I}$. The y -axis of each figure represents the maximum principal angle of a randomly generated subspace with L^* . For each value of the maximum principal angle, the x -axis represents the index in the set of 20 randomly generated subspaces with the specified maximum principal angle. Left: we simulate (21) for the noiseless case $\eta = 0$. Right: Here we add Gaussian noise with variance $\sigma_{\text{noise}}^2 = 10^{-3}$ and simulate (21) with $\eta = 2 \arctan(\sigma_{\text{noise}}) \approx 0.06$.

iteration, and we see that the convergence is linear. The green line denotes the GGD method run with step size $s_{\lfloor k/50 \rfloor} / \sqrt{k}$, where $s_j = 1/(10^j)$. This is motivated by the empirical observation that convergence for the s/\sqrt{k} step size initially experiences fast convergence and then flattens out. The adaptive shrinking of s is able to take advantage of this and makes the convergence rate approximately linear.

7. Conclusion

We have presented a generic condition which ensures that the landscape of the energy function specified by (1) behaves nicely around an underlying subspace: if $\mathcal{S}(\gamma, 0, L^*) > 0$, the underlying subspace is the only minimizer and stationary point in this neighborhood. The generic condition also ensures the convergence of a non-convex gradient method for Robust Subspace Recovery. The method respects the geometry of the Grassmannian manifold by taking gradient steps along geodesics. We have shown that the condition $\mathcal{S} > 0$ probabilistically holds for a given model of data.

More work must go into analysis of the rate of convergence of this algorithm. While in practice we observe linear convergence for line search on nice datasets, such a result seems hard to theoretically justify. We remark that, similar to Lerman and Maunu (2014), we get a sublinear global convergence bound. However, the main point of this work is to get exact recovery guarantees that are similar in spirit to Lerman et al. (2015) for a non-convex algorithm. In fact, it is somewhat surprising that a similar result extends to the non-convex

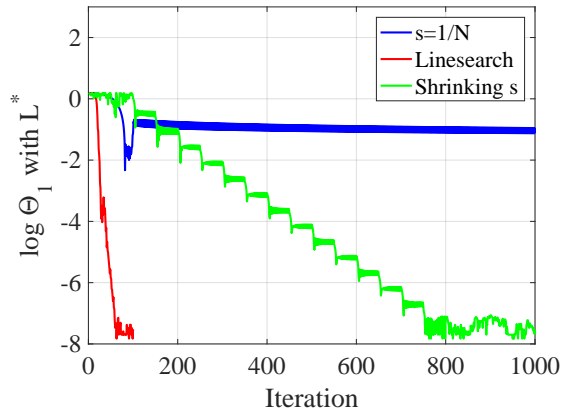


Figure 4: Convergence characteristics of the GGD algorithm with different step size choices. Data was generated according to the Haystack Model. The y -axis is the logarithm of the top principal angle with the underlying subspace L^* .

case. Note that at the subspace itself, our stability is tighter than the stability in Lerman et al. (2015), due to the fact that we do not relax the problem. Our result is weaker, though, due to the fact that it depends on a neighborhood of the underlying subspace. And, though our estimates are slightly worse than Lerman et al. (2015), it is highly nontrivial to extend such probabilistic estimates to the non-convex case. As far as we know, there is no non-convex RSR competitor for the types of estimates we have developed in this paper. Future work will go into improving the bound (14). Based on comparison with Lerman et al. (2015), the bounds do not appear to be ideal, since the non-convex method does not achieve the optimal SNR. Empirically, we have found the geodesic gradient method developed here achieves the same SNR as the state of the art methods displayed in Table 1. However, it is unclear how far we can push the analysis developed here.

We are also interested to know whether one can alleviate the dependence of the conditions in Theorems 5 and 6 on the inlier and outlier variances by introducing spherization into the GGD procedure.

Future work may also consider proof of convergence for other gradient methods, such as Newton’s method, conjugate gradient (Edelman et al., 1999), or IRLS (Lerman and Maunu, 2014), using the guarantees on the energy landscape of this paper. One may also directly follow the ideas of Lim et al. (2016) and consider extensions to the affine Grassmannian, since in practice we cannot assume that the data is properly centered.

Acknowledgments

This work was supported by NSF award DMS-14-18386 and a UMII MnDRIVE graduate assistantship. The authors would like to thank Chao Gao and Nati Srebro for helpful discussion on a preliminary version of the work.

References

- P.-A. Absil, R. Mahony, and R. Sepulchre. Riemannian geometry of Grassmann manifolds with a view on algorithmic computation. *Acta Applicandae Mathematica*, 80(2):199–220, 2004.
- S. Arora, R. Ge, T. Ma, and A. Moitra. Simple, efficient, and neural algorithms for sparse coding. *arXiv preprint arXiv:1503.00778*, 2015.
- N. Boumal. Nonconvex phase synchronization. *arXiv preprint arXiv:1601.06114*, 2016.
- E. J. Candès, X. Li, Y. Ma, and J. Wright. Robust principal component analysis? *Journal of the ACM (JACM)*, 58(3):11, 2011.
- M. Coudron and G. Lerman. On the sample complexity of robust PCA. In *NIPS*, pages 3230–3238, 2012.
- Y. N. Dauphin, R. Pascanu, C. Gulcehre, K. Cho, S. Ganguli, and Y. Bengio. Identifying and attacking the saddle point problem in high-dimensional non-convex optimization. In *NIPS*, pages 2933–2941, 2014.
- C. Davis and W. M. Kahan. The rotation of eigenvectors by a perturbation. iii. *SIAM J. on Numerical Analysis*, 7:1–46, 1970.
- C. Ding, D. Zhou, X. He, and H. Zha. R1-PCA: rotational invariant L_1 -norm principal component analysis for robust subspace factorization. In *ICML*, pages 281–288, 2006.
- A. Edelman, T. A. Arias, and S. T. Smith. The geometry of algorithms with orthogonality constraints. *SIAM J. Matrix Anal. Appl.*, 20(2):303–353, 1999.
- R. Ge, F. Huang, C. Jin, and Y. Yuan. Escaping from saddle pointsonline stochastic gradient for tensor decomposition. In *COLT*, pages 797–842, 2015.
- R. Ge, J. D. Lee, and T. Ma. Matrix completion has no spurious local minimum. In *NIPS*, pages 2973–2981, 2016.
- J. Goes, T. Zhang, R. Arora, and G. Lerman. Robust stochastic principal component analysis. *JMLR W&CP*, page 266274, 2014.
- M. Hardt. Understanding alternating minimization for matrix completion. In *FOCS*, pages 651–660. IEEE, 2014.
- M. Hardt and A. Moitra. Algorithms and hardness for robust subspace recovery. In *COLT*, pages 354–375, 2013.
- P. Jain, A. Tewari, and P. Kar. On iterative hard thresholding methods for high-dimensional m-estimation. In *NIPS*, pages 685–693, 2014.
- I. T. Jolliffe. *Principal Component Analysis*. Springer Series in Statistics. Springer, 2nd edition, 2002.

- B. Laurent and P. Massart. Adaptive estimation of a quadratic functional by model selection. *Annals of Statistics*, pages 1302–1338, 2000.
- J. D. Lee, M. Simchowitz, M. I. Jordan, and B. Recht. Gradient descent only converges to minimizers. In *COLT*, pages 1246–1257, 2016.
- G. Lerman and T. Maunu. Fast, robust and non-convex subspace recovery. *arXiv preprint arXiv:1406.6145*, 2014.
- G. Lerman and T. Zhang. Robust recovery of multiple subspaces by geometric l_p minimization. *Ann. Statist.*, 39(5):2686–2715, 2011.
- G. Lerman and T. Zhang. l_p -recovery of the most significant subspace among multiple subspaces with outliers. *Constructive Approximation*, 40(3):329–385, 2014.
- G. Lerman, M. B. McCoy, J. A. Tropp, and T. Zhang. Robust computation of linear models by convex relaxation. *Foundations of Computational Mathematics*, 15(2):363–410, 2015.
- X. Li and J. Haupt. Identifying outliers in large matrices via randomized adaptive compressive sampling. *Submitted to IEEE Transactions on Signal Processing*, June 2014.
- L. Lim, K. Wong, and K. Ye. Statistical estimation and the affine Grassmannian. *arXiv preprint arXiv:1607.01833*, 2016.
- R. A. Maronna. Principal components and orthogonal regression based on robust scales. *Technometrics*, 47:264–273, 2005.
- R. A. Maronna, R. D. Martin, and V. J. Yohai. *Robust statistics: Theory and methods*. Wiley Series in Probability and Statistics. John Wiley & Sons Ltd., Chichester, 2006.
- M. McCoy and J. Tropp. Two proposals for robust PCA using semidefinite programming. *Elec. J. Stat.*, 5:1123–1160, 2011.
- S. Mei, Y. Bai, and A. Montanari. The landscape of empirical risk for non-convex losses. *arXiv preprint arXiv:1607.06534*, 2016.
- P. Netrapalli, U. Niranjan, S. Sanghavi, A. Anandkumar, and P. Jain. Non-convex robust pca. In *NIPS*, pages 1107–1115, 2014.
- H. Nyquist. Least orthogonal absolute deviations. *Computational Statistics & Data Analysis*, 6(4):361 – 367, 1988.
- M. R. Osborne and G. A. Watson. An analysis of the total approximation problem in separable norms, and an algorithm for the total l_1 problem. *SIAM Journal on Scientific and Statistical Computing*, 6(2):410–424, 1985.
- Mark Rudelson and Roman Vershynin. The littlewoodofford problem and invertibility of random matrices. *Advances in Mathematics*, 218(2):600 – 633, 2008. ISSN 0001-8708. doi: <http://dx.doi.org/10.1016/j.aim.2008.01.010>. URL <http://www.sciencedirect.com/science/article/pii/S0001870808000224>.

- T. Söderström. *Perturbation results for singular values*. Institutionen för informationsteknologi, Uppsala universitet, 1999.
- H. Späth and G. A. Watson. On orthogonal linear ℓ_1 approximation. *Numer. Math.*, 51: 531–543, October 1987.
- J. Sun, Q. Qu, and J. Wright. Complete dictionary recovery over the sphere. In *SampTA*, pages 407–410, May 2015a.
- J. Sun, Q. Qu, and J. Wright. When are nonconvex problems not scary? In *NIPS*, 2015b.
- B. Thomas, L. Lin, L. Lim, and S. Mukherjee. Learning subspaces of different dimension. *arXiv preprint arXiv:1404.6841*, 2014.
- R. Vershynin. How close is the sample covariance matrix to the actual covariance matrix? *Journal of Theoretical Probability*, 25(3):655–686, 2012a.
- R. Vershynin. Introduction to the non-asymptotic analysis of random matrices. In *Compressed sensing*, pages 210–268. Cambridge Univ. Press, Cambridge, 2012b.
- V. Q. Vu, J. Cho, J. Lei, and K. Rohe. Fantope projection and selection: A near-optimal convex relaxation of sparse PCA. In *NIPS*, pages 2670–2678, 2013.
- G. A. Watson. *Some Problems in Orthogonal Distance and Non-Orthogonal Distance Regression*. Defense Technical Information Center, 2001.
- H. Xu, C. Caramanis, and S. Sanghavi. Robust PCA via outlier pursuit. *IEEE Transactions on Information Theory*, 58(5):3047–3064, 2012.
- H. Xu, C. Caramanis, and S. Mannor. Outlier-robust pca: the high-dimensional case. *IEEE Transactions on Information Theory*, 59(1):546–572, 2013.
- K. Ye and L. Lim. Schubert varieties and distances between subspaces of different dimensions. *SIAM Journal on Matrix Analysis and Applications*, 37(3):1176–1197, 2016.
- X. Yi, D. Park, Y. Chen, and C. Caramanis. Fast algorithms for robust pca via gradient descent. In *NIPS*, pages 4152–4160, 2016.
- D. Zhang and L. Balzano. Global convergence of a Grassmannian gradient descent algorithm for subspace estimation. In *AISTATS*, 2016.
- T. Zhang. Robust subspace recovery by Tyler’s M-estimator. *Information and Inference*, 5(1):1–21, 2016.
- T. Zhang and G. Lerman. A novel M-estimator for robust PCA. *JMLR*, 15:749–808, 2014.
- T. Zhang, A. Szlam, and G. Lerman. Median K -flats for hybrid linear modeling with many outliers. In *ICCV*, pages 234–241, 2009.

Appendix A. Grassmannian Geodesics

In this appendix, we describe some basic geometric notions on the Grassmannian manifold, $G(D, d)$. Given two subspaces $L_1, L_2 \in G(D, d)$, the principal angles between the two subspaces are defined sequentially. The smallest angle, θ_d , is given by

$$\theta_d = \min_{\substack{\mathbf{v} \in L_1, \mathbf{y} \in L_2 \\ \|\mathbf{v}\| = \|\mathbf{y}\| = 1}} \arccos(|\mathbf{v}^T \mathbf{y}|). \quad (22)$$

The vectors \mathbf{v}_d and \mathbf{y}_d which achieve the maximum are the principal vectors corresponding to θ_d . The d principal angles are defined sequentially by

$$\theta_k = \min_{\substack{\mathbf{v} \in L_1, \|\mathbf{v}\|=1, \mathbf{v} \perp \mathbf{v}_{k+1}, \dots, \mathbf{v}_d \\ \mathbf{y} \in L_2, \|\mathbf{y}\|=1, \mathbf{y} \perp \mathbf{y}_{d+1}, \dots, \mathbf{y}_d}} \arccos(|\mathbf{v}^T \mathbf{y}|), \quad (23)$$

and the corresponding principal vectors are found in the same way. The ordering defined in (22) and (23) is the reverse of what is usually used for principal angles: here, θ_1 is the largest principal angle, while other works denote the smallest principal angle with θ_1 . Notice that if two principal angles are equal, the choice of principal vectors is not unique. Principal angles and vectors can be efficiently calculated: if $\mathbf{W}_1 \in O(D, d)$ spans L_1 and $\mathbf{W}_2 \in O(D, d)$ spans L_2 , then we write the singular value decomposition

$$\mathbf{W}_1^T \mathbf{W}_2 = \mathbf{V}_{12} \boldsymbol{\Sigma}_{12} \mathbf{Y}_{12}^T. \quad (24)$$

The principal angles are given in reverse order by $\arccos(\text{diag}(\boldsymbol{\Sigma}_{12}))$, and the corresponding principal vectors are given by the columns of \mathbf{V}_{12} and \mathbf{Y}_{12} in reverse order. Now let two subspaces L_1 and L_2 have principal angles $\theta_1, \dots, \theta_d$ and principal vectors $\mathbf{v}_1, \dots, \mathbf{v}_d$ and $\mathbf{y}_1, \dots, \mathbf{y}_d$, respectively. Let k be the last index such that $\theta_k > 0$, which is also known as the interaction number (Lerman and Zhang, 2014). Then, we can define a complementary orthogonal basis $\mathbf{u}_1, \dots, \mathbf{u}_k$ for L_2 with respect to L_1 as

$$\mathbf{u}_j \in \text{Sp}(\mathbf{v}_j, \mathbf{y}_j), \quad \mathbf{u}_j \perp \mathbf{v}_j, \quad \mathbf{u}_j^T \mathbf{y}_j > 0. \quad (25)$$

For any two subspaces L_1 and L_2 such that $\theta_1 = \arccos(|\mathbf{v}_1^T \mathbf{y}_1|) < \pi/2$, a unique geodesic on $G(D, d)$ with $L(0) = L_1$ and $L(1) = L_2$ can be parametrized by

$$L(t) = \text{Sp}(\mathbf{v}_1 \cos(\theta_1 t) + \mathbf{u}_1 \sin(\theta_1 t), \dots, \mathbf{v}_k \cos(\theta_k t) + \mathbf{u}_k \sin(\theta_k t), \mathbf{v}_{k+1}, \dots, \mathbf{v}_d). \quad (26)$$

Appendix B. Proof of Theorem 2

Analogous to the proof of Theorem 1, we will show that, for any $L \in \overline{B(L^*, \sin(\gamma))} \setminus B(L^*, \sin(\eta))$, there is a geodesic $L(t)$ with $L(0) = L$ and an open interval $(0, \delta(L))$ such that

$$F(L(t); \mathcal{X}) < F(L; \mathcal{X}) \text{ and } \Theta_1(L(t), L^*) < \Theta_1(L, L^*), \quad \forall t \in (0, \delta(L)). \quad (27)$$

From the proof of Theorem 1, this implies that local minimizers lie in $B(L^*, \sin(\eta))$.

The rest of the proof largely follows the proof of Theorem 1 in §4.3. Fix a subspace $L \in \overline{B(L^*, \sin(\gamma))} \setminus B(L^*, \sin(\eta))$, and let the principal angles between L and L^* be $\theta_1, \dots, \theta_d$.

Also, choose a set of corresponding principal vectors $\mathbf{v}_1, \dots, \mathbf{v}_d$ and $\mathbf{y}_1, \dots, \mathbf{y}_d$, and let l be the maximum index such that $\theta_1 = \dots = \theta_l$. We let $\mathbf{u}_1, \dots, \mathbf{u}_l$ be complementary orthogonal vectors for $\mathbf{v}_1, \dots, \mathbf{v}_l$ and $\mathbf{y}_1, \dots, \mathbf{y}_l$, which exist since $\Theta_1(L, L^*) > 0$. Parametrize the particular geodesic

$$L(t) = \text{Sp}(\mathbf{v}_1 \cos(t) + \mathbf{u}_1 \sin(t), \dots, \mathbf{v}_l \cos(t) + \mathbf{u}_l \sin(t), \mathbf{v}_{l+1}, \dots, \mathbf{v}_d).$$

This geodesic moves only the furthest directions of $L(0)$ towards L^* , and we have removed dependence on θ_1 , since this unnecessarily impacts the magnitude of the geodesic derivative (4). Then, following (4), we have

$$\begin{aligned} \frac{d}{dt} F(L(t); \mathcal{X}) \Big|_{t=0} &= - \sum_{j=1}^l \sum_{\mathcal{X}} \frac{\mathbf{v}_j^T \mathbf{x}_i \mathbf{x}_i^T \mathbf{u}_j}{\|\mathbf{Q}_L \mathbf{x}_i\|} \\ &= - \sum_{j=1}^l \left(\sum_{\mathcal{X}_1(L^*, \eta)} \frac{\mathbf{v}_j^T \mathbf{x}_i \mathbf{x}_i^T \mathbf{u}_j}{\|\mathbf{Q}_L \mathbf{x}_i\|} + \sum_{\mathcal{X}_0(L^*, \eta)} \frac{\mathbf{v}_j^T \mathbf{x}_i \mathbf{x}_i^T \mathbf{u}_j}{\|\mathbf{Q}_L \mathbf{x}_i\|} \right) \\ &\leq - \sum_{j=1}^l \left(\cos(\gamma + \eta) \cos(\eta) \sum_{\mathcal{X}_1(L^*, \eta)} \frac{\mathbf{y}_j^T \mathbf{x}_i \mathbf{x}_i^T \mathbf{y}_j}{\|\mathbf{x}_i\|} - \max_{\mathbf{V} \in \overline{B(L^*, \sin(\gamma))}} \sigma_1(\nabla F(\mathbf{V}; \mathcal{X}_0(L^*, \eta))) \right) \\ &\leq -l\mathcal{S}(\gamma, \eta, L^*) < -\mathcal{S}(\gamma, \eta, L^*) < 0. \end{aligned} \tag{28}$$

Thus, (28) implies that every subspace in $\overline{B(L^*, \sin(\gamma))} \setminus \overline{B(L^*, \sin(\eta))}$ has a direction with negative local subderivative.

If $l < d$, then let $\delta(L) = \theta_l - \theta_{l+1}$, and otherwise let $\delta(L) = \theta_l$. Then, notice that for all $L(\tilde{t})$, $\tilde{t} \in (-\pi/2 + \gamma, \delta(L))$, we have the same bound

$$\frac{d}{dt} F(L(t); \mathcal{X}) \Big|_{t=\tilde{t}} < -\mathcal{S}(\gamma, \eta, L^*) < 0.$$

This means that at $L(0)$, the subdifferential is bounded above by $-\mathcal{S}(\gamma, \eta, L^*)$. This follows from the fact that the one-dimensional continuous function $F(L(t); \mathcal{X})$ has subdifferential at $L(0)$ bounded by the maximum subderivatives of $F(L(t); \mathcal{X})$ as $t \rightarrow 0^\pm$. Thus, we have proven (27), since $F(L(t); \mathcal{X})$ must be decreasing on $(0, \delta(L))$.

Appendix C. Proof of Theorem 3

We will first show that

$$\Theta_1(\mathbf{V}^{k+1}, L^*) < \Theta_1(\mathbf{V}^k, L^*), \tag{29}$$

for sufficiently small t^k . Let $\mathbf{V}^* \in O(D, d)$ span L^* . We will establish (29) by showing

$$\sigma_d(\mathbf{V}^{*T} \mathbf{V}^{k+1}) > \sigma_d(\mathbf{V}^{*T} \mathbf{V}^k).$$

Using (13) and the fact that

$$\cos(\boldsymbol{\Sigma}^k t^k) = \mathbf{I} - O((t^k)^2), \quad \sin(\boldsymbol{\Sigma}^k t^k) = \boldsymbol{\Sigma}^k t^k - O((t^k)^3),$$

we can write

$$\begin{aligned}\sigma_d\left(\mathbf{V}^{*T}\mathbf{V}^{k+1}\right) &= \sigma_d\left(\mathbf{V}^{*T}\left(\mathbf{V}^k\mathbf{W}^k\cos(\boldsymbol{\Sigma}^k t^k)\mathbf{W}^{kT} + \mathbf{U}^k\sin(\boldsymbol{\Sigma}^k t^k)\mathbf{W}^{kT}\right)\right) \\ &= \sigma_d\left(\mathbf{V}^{*T}\left(\mathbf{V}^k - t^k\nabla F(\mathbf{V}^k; \mathcal{X}) + O((t^k)^2)\right)\right).\end{aligned}\quad (30)$$

Let $\mathbf{v}_1^k \in \text{Sp}(\mathbf{V}^k)$ be a unit vector corresponding to the maximum principal angle with L^* , and let \mathbf{u}_1^k be its complementary orthogonal vector. Define the unit vector $\mathbf{y}_1^k \in L^* \cap \text{Sp}(\mathbf{v}_1^k, \mathbf{u}_1^k)$, and write $\theta_1^k = \Theta_1(\text{Sp}(\mathbf{V}^k), L^*)$. Let $\|\boldsymbol{\beta}_1\| = \|\boldsymbol{\beta}_2\| = 1$ be such that

$$\boldsymbol{\beta}_1^T \mathbf{V}^{*T} \mathbf{V}^k \boldsymbol{\beta}_2 = \sigma_d(\mathbf{V}^{*T} \mathbf{V}^k). \quad (31)$$

Then, we have $\boldsymbol{\beta}_1^T \mathbf{V}^{*T} = \mathbf{y}_1^{kT}$ and $\mathbf{V}^k \boldsymbol{\beta}_2 = \mathbf{v}_1^k$.

We now apply Result 4.1 in Söderström (1999), which states the following. Suppose a matrix \mathbf{A} has a singular value σ with multiplicity r , with corresponding left and right singular vectors \mathbf{U} and \mathbf{V} . Suppose that we perturb \mathbf{A} by $\epsilon \mathbf{B}$. Then, $\mathbf{A} + \epsilon \mathbf{B}$ has r singular values $\sigma_1(\mathbf{A} + \epsilon \mathbf{B}), \dots, \sigma_r(\mathbf{A} + \epsilon \mathbf{B})$ which satisfy

$$\sigma_j(\mathbf{A} + \epsilon \mathbf{B}) = \sigma_j(\mathbf{A}) + \frac{\epsilon}{2} \lambda_j(\mathbf{V}^T \mathbf{B}^T \mathbf{U} + \mathbf{U}^T \mathbf{B} \mathbf{V}) + O(\epsilon^2).$$

Applying this to (30) yields

$$\begin{aligned}\sigma_d\left(\mathbf{V}^{*T}\mathbf{V}^{k+1}\right) &= \sigma_d\left(\mathbf{V}^{*T}\mathbf{V}^k\right) + t^k \left(\boldsymbol{\beta}_1^T \mathbf{V}^{*T} \sum_{\mathcal{X}} \frac{\mathbf{Q}_{\mathbf{V}^k} \mathbf{x}_i \mathbf{x}_i^T \mathbf{V}^k}{\|\mathbf{Q}_{\mathbf{V}^k} \mathbf{x}_i\|} \boldsymbol{\beta}_2 \right) + O((t^k)^2) \\ &= \sigma_d\left(\mathbf{V}^{*T}\mathbf{V}^k\right) + t^k \left(\mathbf{y}_1^{kT} \sum_{\mathcal{X}} \frac{\mathbf{Q}_{\mathbf{V}^k} \mathbf{x}_i \mathbf{x}_i^T}{\|\mathbf{Q}_{\mathbf{V}^k} \mathbf{x}_i\|} \mathbf{v}_1^k \right) + O((t^k)^2) \\ &= \sigma_d\left(\mathbf{V}^{*T}\mathbf{V}^k\right) + t^k \sin(\theta_1^k) \left(\mathbf{u}_1^{kT} \sum_{\mathcal{X}_1} \frac{\mathbf{x}_i \mathbf{x}_i^T}{\|\mathbf{Q}_{\mathbf{V}^k} \mathbf{x}_i\|} \mathbf{v}_1^k + \mathbf{u}_1^{kT} \sum_{\mathcal{X}_0} \frac{\mathbf{x}_i \mathbf{x}_i^T}{\|\mathbf{Q}_{\mathbf{V}^k} \mathbf{x}_i\|} \mathbf{v}_1^k \right) + O((t^k)^2).\end{aligned}\quad (32)$$

Here, the $O((t^k)^2)$ term is bounded below by $-C_2(t^k)^2$, where C_2 does not depend on \mathbf{V}^k , which follows from compactness of $O(D, d)$.

Notice that the inlier term in (32) is positive and bounded below

$$\begin{aligned}\mathbf{u}_1^{kT} \sum_{\mathcal{X}_1} \frac{\mathbf{x}_i \mathbf{x}_i^T}{\|\mathbf{Q}_{\mathbf{V}^k} \mathbf{x}_i\|} \mathbf{v}_1^k &\geq \frac{1}{\sin(\Theta_1(\text{Sp}(\mathbf{V}^k), L^*))} \sum_{\mathcal{X}_1} \frac{\mathbf{u}_1^{kT} \mathbf{x}_i \mathbf{x}_i^T \mathbf{v}_1^k}{\|\mathbf{x}_i\|} \\ &\geq \cos(\Theta_1(\text{Sp}(\mathbf{V}^k), L^*)) \sum_{\mathcal{X}_1} \frac{\mathbf{y}_1^{kT} \mathbf{x}_i \mathbf{x}_i^T \mathbf{y}_1^k}{\|\mathbf{x}_i\|} \geq \cos(\gamma) \lambda_d \left(\sum_{\mathcal{X}_1} \frac{\mathbf{x}_i \mathbf{x}_i^T}{\|\mathbf{x}_i\|} \right).\end{aligned}\quad (33)$$

Using the fact that $\mathbf{u}_1^k \in \text{Sp}(\mathbf{Q}_{\mathbf{V}^k})$ and $\mathbf{v}_1^k \in \text{Sp}(\mathbf{V}^k)$, we can bound the outlier term in (32)

$$\left| \mathbf{u}_1^{kT} \sum_{\mathcal{X}_0} \frac{\mathbf{x}_i \mathbf{x}_i^T}{\|\mathbf{Q}_{\mathbf{V}^k} \mathbf{x}_i\|} \mathbf{v}_1^k \right| \leq \sigma_1 \left(\sum_{\mathcal{X}_0} \frac{\mathbf{Q}_{\mathbf{V}^k} \mathbf{x}_i \mathbf{x}_i^T}{\|\mathbf{Q}_{\mathbf{V}^k} \mathbf{x}_i\|} \mathbf{V}^k \right) = \sigma_1 \left(\nabla F(\mathbf{V}^k; \mathcal{X}_0) \right). \quad (34)$$

Thus, from (33) and (34) we conclude

$$\begin{aligned}
& \sigma_d(\mathbf{V}^{*T}\mathbf{V}^{k+1}) - \sigma_d(\mathbf{V}^{*T}\mathbf{V}^k) \\
& \geq t^k \sin(\theta_1^k) \left(\cos(\gamma)\lambda_d \left(\sum_{\mathcal{X}_1} \frac{\mathbf{x}_i \mathbf{x}_i^T}{\|\mathbf{x}_i\|} \right) - \sigma_1(\nabla F(\mathbf{V}^k; \mathcal{X}_0)) \right) - C_2(t^k)^2 \\
& \geq t^k \sin(\theta_1^k) \left(\cos(\gamma)\lambda_d \left(\sum_{\mathcal{X}_1} \frac{\mathbf{x}_i \mathbf{x}_i^T}{\|\mathbf{x}_i\|} \right) - \max_{\mathbf{V} \in B(L^*, \sin(\gamma))} \sigma_1(\nabla F(\mathbf{V}; \mathcal{X}_0)) \right) - C_2(t^k)^2 \\
& \geq t^k \sin(\theta_1^k) C_1 - C_2(t^k)^2 = t^k \left(\sin(\theta_1^k) C_1 - C_2 t^k \right),
\end{aligned} \tag{35}$$

for positive constants C_1 and C_2 which do not depend on \mathbf{V}^k . Hence, for small enough t^k , we have that (29) holds. It remains to show that the sequence with step size s/\sqrt{k} converges to L^* for sufficiently small s . Suppose that s satisfies

$$s < \min \left(\frac{C_1 \sin(\gamma)}{2C_2}, \frac{1}{4\sqrt{C_2}} \right). \tag{36}$$

Then, for any \mathbf{V}^k with $\frac{\gamma}{2\sqrt{k}} \leq \Theta_1(\mathbf{V}^k, L^*) \leq \gamma$, looking at (35) and the first term in (36), s/\sqrt{k} decreases the principal angle by at least C_3/k , for some constant C_3 . On the other hand, for any \mathbf{V}^k such that $\Theta_1(\mathbf{V}^k, L^*) < \frac{\gamma}{2\sqrt{k}}$, we have the bound

$$\sigma_d(\mathbf{V}^{*T}\mathbf{V}^{k+1}) - \sigma_d(\mathbf{V}^{*T}\mathbf{V}^k) > -C_2(t^k)^2. \tag{37}$$

Note that (37) gives the inequality

$$\sigma_d(\mathbf{V}^{*T}\mathbf{V}^{k+1}) > \sigma_d(\mathbf{V}^{*T}\mathbf{V}^k) - C_2(t^k)^2 \geq \cos\left(\frac{\gamma}{2\sqrt{k}}\right) - C_2(t^k)^2. \tag{38}$$

It is straightforward to show that if

$$t^k < \frac{1}{4\sqrt{C_2}\sqrt{k}},$$

then the right hand side of (38) is greater than $\cos(\gamma/\sqrt{k})$. Thus, the second term in the minimum of (36) implies that if $\Theta_1(\mathbf{V}^k, L^*) < \frac{\gamma}{2\sqrt{k}}$, then $\Theta_1(\mathbf{V}^{k+1}, L^*) < \gamma/\sqrt{k}$.

We summarize this in the following way. For any k , either $\frac{\gamma}{2\sqrt{k}} \leq \Theta_1(\mathbf{V}^k, L^*) \leq \gamma$ or $\Theta_1(\mathbf{V}^k, L^*) < \frac{\gamma}{2\sqrt{k}}$. If the former holds, then $\Theta_1(\mathbf{V}^{k+1}, L^*) < \Theta_1(\mathbf{V}^k, L^*) - C_3/k$. If the latter holds, then we have the bound $\Theta_1(\mathbf{V}^{k+1}, L^*) < \gamma/\sqrt{k}$. Thus, the maximum principal angle with L^* either decreases by C_3/k or the distance is bounded by γ/\sqrt{k} . Put together, these imply that \mathbf{V}^k converges to L^* with $O(1/\sqrt{k})$ rate of convergence.

Appendix D. Proof of Theorem 4

Suppose that $\mathbf{V}^k \in \overline{B(L^*, \sin(\gamma)) \setminus B(L^*, \sin(\eta))}$ and that $\mathcal{S}(\gamma, \eta, L^*) > 0$. Then, following the proof of Theorem 3, we see that equations (30)-(32) hold. We must modify the bound in (33). Let \mathbf{v}_1^k be the vector corresponding to the maximum principal angle of \mathbf{V}^k with L^* and let \mathbf{u}_1^k be its complementary orthogonal vector with respect to L^* . Let $\theta_1^k = \Theta_1(\mathbf{V}^k, L^*)$. We must show that

$$\mathbf{u}_1^{kT} \sum_{\mathcal{X}_1(L^*, \eta)} \frac{\mathbf{x}_i \mathbf{x}_i^T}{\|\mathbf{Q}_{\mathbf{V}^k} \mathbf{x}_i\|} \mathbf{v}_1^k + \mathbf{u}_1^{kT} \sum_{\mathcal{X}_0(L^*, \eta)} \frac{\mathbf{x}_i \mathbf{x}_i^T}{\|\mathbf{Q}_{\mathbf{V}^k} \mathbf{x}_i\|} \mathbf{v}_1^k > 0. \quad (39)$$

On the one hand, since $\theta_1^k > \eta$,

$$\mathbf{u}_1^{kT} \frac{\mathbf{x}_i \mathbf{x}_i^T}{\|\mathbf{Q}_{\mathbf{V}^k} \mathbf{x}_i\|} \mathbf{v}_1^k > 0, \quad \forall \mathbf{x}_i \in \mathcal{X}_1(L^*, \eta). \quad (40)$$

For each $\mathbf{x}_i \in \mathcal{X}_1(L^*, \eta)$, let $\angle_i = \angle(\mathbf{x}_i, L^*)$. The following two bounds hold for all $\mathbf{x}_i \in \mathcal{X}_1(L^*, \eta)$:

$$\|\mathbf{Q}_{\mathbf{V}^k} \mathbf{x}_i\| \leq \sin(\theta_1^k + \angle_i) \|\mathbf{x}_i\|, \quad (41)$$

$$\mathbf{u}_1^{kT} \mathbf{x}_i \mathbf{x}_i^T \mathbf{v}_1^k \geq \cos(\theta_1^k + \angle_i) \sin(\theta_1^k + \angle_i) \mathbf{y}_1^{kT} \mathbf{x}_i \mathbf{x}_i^T \mathbf{y}_1^k. \quad (42)$$

Inequalities (40), (41), and (42) imply that

$$\begin{aligned} \mathbf{u}_1^{kT} \sum_{\mathcal{X}_1(L^*, \eta)} \frac{\mathbf{x}_i \mathbf{x}_i^T}{\|\mathbf{Q}_{\mathbf{V}^k} \mathbf{x}_i\|} \mathbf{v}_1^k &\geq \sum_{\mathcal{X}_1(L^*, \eta)} \mathbf{y}_1^{kT} \frac{\mathbf{x}_i \mathbf{x}_i^T}{\|\mathbf{x}_i\|} \mathbf{y}_1^k \cos(\theta_1^k + \angle_i) \\ &\geq \lambda_d \left(\sum_{\mathcal{X}_1(L^*, \eta)} \frac{\mathbf{P}_{L^*} \mathbf{x}_i \mathbf{x}_i^T \mathbf{P}_{L^*}}{\|\mathbf{P}_{L^*} \mathbf{x}_i\|} \cos(\theta_1^k + \angle_i) \cos(\angle_i) \right) \\ &\geq \cos(\gamma + \eta) \cos(\eta) \lambda_d \left(\sum_{\mathcal{X}_1(L^*, \eta)} \frac{\mathbf{P}_{L^*} \mathbf{x}_i \mathbf{x}_i^T \mathbf{P}_{L^*}}{\|\mathbf{P}_{L^*} \mathbf{x}_i\|} \right). \end{aligned} \quad (43)$$

As we can see, the last term in (43) is the first term in $\mathcal{S}(\gamma, \eta, L^*)$. For the outlier term, we see that (34) holds. Putting these two together, if $\mathcal{S}(\gamma, \eta, L^*) > 0$, then (39) holds, and thus $\mathcal{S}(\gamma, \eta, L^*) > 0$ is a sufficient condition for the decrease of $\Theta_1(\mathbf{V}^k, L^*)$. The proof of convergence by selecting the correct initial step size follows from the same argument as that in the proof of Theorem 3 (see Appendix C).

Appendix E. Bound on the Alignment

Here we derive the simple bound on the alignment statistic seen in (9). This bound is used to prove Theorems 5 and 7.

$$\begin{aligned}
\mathcal{A}(\mathcal{X}_0, \mathbf{V}) &= \sigma_1 \left(\sum_{\substack{\mathbf{x}_i \in \mathcal{X}_0 \\ \|\mathbf{Q}_\mathbf{V} \mathbf{x}_i\| > 0}} \frac{\mathbf{Q}_\mathbf{V} \mathbf{x}_i}{\|\mathbf{Q}_\mathbf{V} \mathbf{x}_i\|} \mathbf{x}_i^T \mathbf{V} \right) = \max_{\|\mathbf{u}\|=\|\mathbf{w}\|=1} \mathbf{u}^T \sum_{\substack{\mathbf{x}_i \in \mathcal{X}_0 \\ \|\mathbf{Q}_\mathbf{V} \mathbf{x}_i\| > 0}} \frac{\mathbf{Q}_\mathbf{V} \mathbf{x}_i}{\|\mathbf{Q}_\mathbf{V} \mathbf{x}_i\|} \mathbf{x}_i^T \mathbf{V} \mathbf{w} \quad (44) \\
&= \max_{\|\mathbf{u}\|=\|\mathbf{w}\|=1} \sum_{\substack{\mathbf{x}_i \in \mathcal{X}_0 \\ \|\mathbf{Q}_\mathbf{V} \mathbf{x}_i\| > 0}} \mathbf{u}^T \frac{\mathbf{Q}_\mathbf{V} \mathbf{x}_i}{\|\mathbf{Q}_\mathbf{V} \mathbf{x}_i\|} \mathbf{x}_i^T \mathbf{V} \mathbf{w} \leq \max_{\|\mathbf{w}\|=1} \sum_{\substack{\mathbf{x}_i \in \mathcal{X}_0 \\ \|\mathbf{Q}_\mathbf{V} \mathbf{x}_i\| > 0}} |\mathbf{x}_i^T \mathbf{V} \mathbf{w}| \\
&\leq \max_{\mathbf{v} \in S^{D-1}} \sum_{\mathbf{x}_i \in \mathcal{X}_0, \|\mathbf{Q}_\mathbf{V} \mathbf{x}_i\| > 0} |\mathbf{x}_i^T \mathbf{v}| \leq \max_{\mathbf{v} \in S^{D-1}} \|\mathbf{X}_0^T \mathbf{v}\|_1 \\
&\leq \sqrt{N_{\text{out}}} \max_{\mathbf{v} \in S^{D-1}} \|\mathbf{X}_0^T \mathbf{v}\|_2 \leq \sqrt{N_{\text{out}}} \|\mathbf{X}_0\|_2.
\end{aligned}$$

Appendix F. Proof of Theorem 6

To prove this theorem, we only need to show that PCA initializes in $\overline{B(L^*, \sin(\gamma))}$. Note that the covariance matrix for the data \mathcal{X} is $\Sigma = N_{\text{out}} \Sigma_{\text{out}} / (ND_{\text{out}}) + N_{\text{in}} \Sigma_{\text{in}} / (Nd)$. We want to see how close the sample covariance approximates Σ_{in} , since the PCA subspace is spanned by the top d eigenvectors of the sample covariance. Denoting the sample covariance by Σ_N , let \mathbf{V}_{PCA} be its top d eigenvectors. Also, let \mathbf{V}^* be the top d eigenvectors of Σ_{in} and let \mathbf{V} be the top d eigenvectors of Σ . We note that

$$|\sin(\Theta_1(\mathbf{V}_{PCA}, \mathbf{V}^*))| \leq |\sin(\Theta_1(\mathbf{V}_{PCA}, \mathbf{V}))| + |\sin(\Theta_1(\mathbf{V}, \mathbf{V}^*))|. \quad (45)$$

To deal with the last term in (45), the Davis-Kahan $\sin \theta$ Theorem (Davis and Kahan, 1970), or more precisely Corollary 3.1 of Vu et al. (2013), gives

$$|\sin(\Theta_1(\mathbf{V}, \mathbf{V}^*))| \leq \sqrt{2} \frac{\lambda_1(N_{\text{out}} \Sigma_{\text{out}} / (ND_{\text{out}}))}{\lambda_d(N_{\text{in}} \Sigma_{\text{in}} / (Nd))} = \sqrt{2} \frac{N_{\text{out}}}{N_{\text{in}}} \frac{d}{D_{\text{out}}} \frac{\lambda_1(\Sigma_{\text{out}})}{\lambda_d(\Sigma_{\text{in}})}.$$

Thus,

$$\sin(\gamma) > \sqrt{2} \frac{N_{\text{out}}}{N_{\text{in}}} \frac{d}{D_{\text{out}}} \frac{\lambda_1(\Sigma_{\text{out}})}{\lambda_d(\Sigma_{\text{in}})} \quad (46)$$

is a sufficient condition for $|\sin(\Theta_1(\mathbf{V}, \mathbf{V}^*))| < \sin(\gamma)$.

On the other hand, for the first term in the right hand side of (45), we must bound how close the sample covariance is to the true covariance. Proposition 2.1 of Vershynin (2012a) states that

$$\|\Sigma - \Sigma_N\|_2 \leq \epsilon(\delta, \Sigma_{\text{in}}, \Sigma_{\text{out}}) \left(\frac{D_{\text{out}}}{N} \right)^{\frac{1}{2}}, \quad (47)$$

with probability at least $1 - \delta$, where $\epsilon(\delta, \Sigma_{\text{in}}, \Sigma_{\text{out}})$ is a constant depending on δ , Σ_{in} , and Σ_{out} . By assumption, Σ has a positive d th eigengap. Thus, another application of the

Davis-Kahan $\sin \theta$ Theorem yields

$$|\sin(\Theta_1(\mathbf{V}_{PCA}, \mathbf{V}))| \leq \frac{\|\boldsymbol{\Sigma} - \boldsymbol{\Sigma}_N\|_2}{\lambda_d(\boldsymbol{\Sigma}) - \lambda_{d+1}(\boldsymbol{\Sigma})} \leq \epsilon_2(\delta, \boldsymbol{\Sigma}_{\text{in}}, \boldsymbol{\Sigma}_{\text{out}}) \left(\frac{dD}{N}\right)^{\frac{1}{2}},$$

with probability $1 - \delta$. For large enough N , we have

$$|\sin(\Theta_1(\mathbf{V}_{PCA}, \mathbf{V}))| \leq \sin(\gamma) - |\sin(\Theta_1(\mathbf{V}, \mathbf{V}^*))|. \quad (48)$$

Rearranging (48) and using the triangle inequality in (45) yields

$$|\sin(\Theta_1(\mathbf{V}_{PCA}, \mathbf{V}^*))| \leq \sin(\gamma),$$

with probability $1 - \delta$.

Appendix G. Proof of Theorem 7

First, we will show that all the inlier points are in $\mathcal{X}_1(L^*, \eta)$ with high probability. Using Lemma 1 in Laurent and Massart (2000), for any fixed constant b ,

$$\Pr \left((D-d) \frac{\|\boldsymbol{\epsilon}_i\|^2}{\sigma_{\text{noise}}^2 \|\mathbf{x}_i^{L^*}\|^2} \geq (1 + 2\sqrt{b} + b)(D-d) \left| \mathbf{x}_i^{L^*} \right. \right) \leq e^{-b(D-d)}.$$

This simplifies to

$$\Pr \left(\frac{\|\boldsymbol{\epsilon}_i\|}{\|\mathbf{x}_i^{L^*}\|} \geq \sigma_{\text{noise}} \sqrt{1 + 2\sqrt{b} + b} \left| \mathbf{x}_i^{L^*} \right. \right) \leq e^{-C(D-d)}. \quad (49)$$

Taking a union bound over all inlier points, (49) implies

$$\Pr \left(\max_i \frac{\|\boldsymbol{\epsilon}_i\|}{\|\mathbf{x}_i^{L^*}\|} \geq \sigma_{\text{noise}} \sqrt{1 + 2\sqrt{b} + b} \left| \mathbf{x}_1^{L^*}, \dots, \mathbf{x}_{N_{\text{in}}}^{L^*} \right. \right) \leq N_{\text{in}} e^{-b(D-d)}. \quad (50)$$

Thus for $\eta = \sigma_{\text{noise}} \sqrt{1 + 2\sqrt{b} + b}$, then (50) implies that $\mathcal{X}_1 \subset \mathcal{X}_1(L^*, \eta)$ with probability at least $1 - N_{\text{in}} e^{-b(D-d)}$.

Now we estimate the permeance and the alignment. For the alignment, we use the same bound as in the proof of Theorem 5. By Proposition B.3 of Lerman et al. (2015), we can bound the outliers by

$$\begin{aligned} \sqrt{|\mathcal{X}_0(L^*, \eta)|} \|\mathbf{X}_0^\eta\|_2 &\leq \sqrt{N_{\text{out}}} \|\mathbf{X}_0\|_2 \\ &\leq \sigma_{\text{out}} \sqrt{N_{\text{out}}} \left[\sqrt{\frac{N_{\text{out}}}{D}} + 1 + \sqrt{\frac{2C_0}{D}} \right], \text{ w.p. at least } 1 - e^{-C_0}. \end{aligned} \quad (51)$$

On the other hand, if $\mathcal{X}_1 \subset \mathcal{X}_1(L^*, \eta)$, we have a similar bound as before

$$\begin{aligned} \lambda_d \left(\sum_{\mathcal{X}_1(L^*, \eta)} \frac{\mathbf{P}_{L^*} \mathbf{x}_i \mathbf{x}_i^T \mathbf{P}_{L^*}}{\|\mathbf{P}_{L^*} \mathbf{x}_i\|} \right) &\geq \lambda_d \left(\sum_{\mathcal{X}_1} \frac{\mathbf{P}_{L^*} \mathbf{x}_i \mathbf{x}_i^T \mathbf{P}_{L^*}}{\|\mathbf{P}_{L^*} \mathbf{x}_i\|} \right) \\ &\geq \sigma_{\text{in}} \sqrt{d} \left((1-a) \sqrt{\frac{N_{\text{in}}}{d}} - C_1 \right)^2, \text{ w.p. } 1 - 2e^{-c_1 a^2 N_{\text{in}}}. \end{aligned} \quad (52)$$

Thus, we obtain (19) by comparing the right hand side of (52) to the right hand side of (51).